Neotropical Ichthyology

Original article

https://doi.org/10.1590/1982-0224-2026-0077

urn:lsid:zoobank.org:pub:9090FE0A-2417-4EE8-92EA-B3CD8FB40010

Two co-mimic new species of Corydoradinae catfishes (Siluriformes: Callichthyidae) from the rio Tapajós basin, Brazil, with a discussion on their color pattern

Correspondence:
Luiz Fernando Caserta Tencatt
luiztencatt@hotmail.com

Luiz Fernando Caserta Tencatt[1], Willian Massaharu Ohara[2], Vandergleison de Carvalho[3], Steven Grant[1] and Marcelo R. Britto[3]

A crowdfunding initiative carried out by aquarists allowed us to sample tributaries of the rio Tapajós in the surroundings of Jacareacanga City, southwest of Pará State, Brazilian Amazon. In this article, we formally describe two of the captured species, which were found in syntopy, forming a Müllerian mimicry ring. The new *Brochis* can be distinguished from its congeners by the following combination of features: a mask-like blotch; absence of a large dark patch around dorsal-fin base; absence of dark stripes on flanks; caudal fin devoid of conspicuous dark markings; and flanks with dark blotches slightly darker than the ground color of plates. The new *Hoplisoma* can be distinguished from its congeners by the following combination of features: belly with mosaic-like platelets; a mask-like blotch; absence of dark stripes on flanks; absence of a large dark patch around dorsal-fin base; infraorbital 2 in direct contact with pterotic-extrascapular, or at least with its posterodorsal edge clearly surpassing the suture between sphenotic and pterotic-extrascapular; absence of conspicuous dark markings on caudal fin; and flanks with dark blotches slightly darker than the ground color of plates. Considering their unusual color pattern, a discussion on its possible adaptive value of their color patterns is provided. Identification key to the valid species of Corydoradinae from the rio Tapajós basin is provided.

Keywords: Amazon, *Brochis* sp. CW101, *Hoplisoma* sp. CW102, Osteology, Taxonomy.

Submitted May 11, 2026
Accepted August 15, 2026
Epub ???, 2026

Associate Editor Carlos DoNascimiento
Section Editor William Crampton
Editor-in-chief José Birindelli

Online version ISSN 1982-0224
Print version ISSN 1679-6225

Neotrop. Ichthyol.
vol. 24, no. 4, 2026

1 Instituto de Biociências, Universidade Federal de Mato Grosso do Sul, Av. Costa e Silva, s/nº, Bairro Universitário, 79070-900, Campo Grande, MS, Brazil. (LFCT) luiztencatt@hotmail.com (corresponding author), (SG) daroneth@aol.co.uk.

2 Instituto de Ciências Biológicas, Universidade Federal do Amazonas, Av. Rodrigo Otávio Japiim, 69077-000, Manaus, AM, Brazil. (WMO) ohara@ufam.edu.br.

3 Universidade Federal do Rio de Janeiro, Museu Nacional, Departamento de Vertebrados, Setor de Ictiologia, Quinta da Boa Vista, s/n, São Cristóvão, 20940-040, Rio de Janeiro, RJ, Brazil. (VC) dcarvalhojet@hotmail.com, (MRB) mrbritto@mn.ufrj.br.

Uma iniciativa de financiamento coletivo realizada por aquaristas nos permitiu coletar amostras em afluentes do rio Tapajós, nos arredores da cidade de Jacareacanga, sudoeste do estado do Pará, Amazônia brasileira. Neste artigo, descrevemos formalmente duas das espécies capturadas, que foram encontradas em sintopia, formando um anel de mimetismo Mülleriano. A nova espécie de *Brochis* pode ser distinguida de suas congêneres pela seguinte combinação de características: uma mancha em forma de máscara; ausência de uma grande mancha escura ao redor da base da nadadeira dorsal; ausência de faixas escuras nos flancos; nadadeira caudal desprovida de marcas escuras conspícuas; flancos com manchas escuras ligeiramente mais escuras que a cor de fundo das placas. A nova *Hoplisoma* pode ser distinguida de suas congêneres pela seguinte combinação de características: ventre com plaquetas em mosaico; uma mancha em forma de máscara; ausência de faixas escuras nos flancos; ausência de uma grande mancha escura ao redor da base da nadadeira dorsal; infraorbital 2 em contato direto com a pterótico-extrascapular, ou pelo menos com sua borda póstero-dorsal ultrapassando claramente a sutura entre a esfenótico e a pterótico-extrascapular; ausência de marcas escuras conspícuas na nadadeira caudal; e flancos com manchas escuras ligeiramente mais escuras que a cor de fundo das placas. Considerando seu padrão de coloração incomum, discute-se seu possível valor adaptativo positivo. É apresentada uma chave de identificação para as espécies válidas de Corydoradinae da bacia do rio Tapajós.

Palavras-chave: Amazônia, *Brochis* sp. CW101, *Hoplisoma* sp. CW102, Osteologia, Taxonomia.

INTRODUCTION

The Callichthyidae catfishes can be distinguished from the remaining Siluriformes by having two longitudinal series of dermal plates on the flanks (Reis, 1998, 2003). Currently, the family harbors around 230 valid species distributed in two subfamilies, Callichthyinae, with five valid genera, and Corydoradinae, with seven valid genera (Dias *et al*., 2025; Fricke *et al*., 2026). Callichthyinae is composed by small- to medium-sized callichtyids (up to about 150.0 mm SL) with long maxillary barbel (at least reaching the pectoral-fin origin), while the Corydoradinae harbors small-sized corydoradines (up to about 100 mm SL) with short maxillary barbel (not reaching the pectoral-fin origin) (Britto *et al*., 2025). Currently, Callichthyinae encompasses 17 valid species, whereas Corydoradinae around 210 valid species, representing *circa* 9% and 91% of the diversity of the family, respectively.

Hoplisoma sensu Dias *et al.* (2025) is currently the most species-rich genus within Corydoradinae, and also from Callichthyidae, with about 90 valid species, followed by *Brochis*, with more than 40 valid species. The species of *Hoplisoma* can be recognized by sharing the following non-exclusive features: (I) mesethmoid moderate in size, (II) posterior margin of both dorsal- and pectoral-fin spines typically with all or nearly all serrations directed towards the tip of the spine or perpendicularly directed, (III)

posterior laminar expansion of infraorbital 2 ranging from strongly reduced to relatively well developed, typically not in contact with pterotic-extrascapular, (IV) single cranial fontanel, and (V) a combination of ground color of body pale yellow, brownish yellow or grayish yellow, typically with small dark spots at least in some part of the body and/or more than one large, dark blotch/stripe on body (Dias *et al*., 2025; Tencatt *et al*., 2025a). On the other hand, the species of *Brochis* in the revised concept by Dias *et al.* (2025) can be promptly distinguished from the remaining Corydoradinae by having two exclusive features, (I) posterior margin of both dorsal and pectoral spines mostly covered by laminar/blade-like serrations, and (II) posterior margin of dorsal-fin spine with retrorse serrations.

As previously discussed, the flow of putatively undescribed species of Corydoradinae in the aquarium trade is remarkable, especially when considering the rio Amazonas basin (see Tencatt *et al*., 2021, 2022a, 2023a,b, 2024a,b, 2025a,b). Among the tributaries of the Amazon basin reported to have a considerably high number of new Corydoradinae species stands the rio Tapajós, which currently harbors eight valid species of *Hoplisoma*, namely: *H. apiaka* (Espíndola, Spencer, Rocha & Britto, 2014), *H. benattii* (Espíndola, Tencatt, Pupo, Villa-Verde & Britto, 2018), *H. hypnos* (Tencatt, Ohara, Sousa & Britto, 2022), *H. noxium* Tencatt, Ohara, Carvalho, Grant & Britto, 2025, *H. psamathos* (Tencatt, Ohara, Sousa & Britto, 2022), *H. rikbaktsa* (Lima & Britto, 2020), *H. tenebrosum* Tencatt, Ohara, Carvalho, Grant & Britto, 2025, *H. thanatos* (Tencatt, Ohara, Sousa & Britto, 2022), and 12 putatively undescribed species recognized in the aquarium trade by the following codes: *Hoplisoma* sp. C133, CW102, CW127, CW162, CW171, CW187, CW191, CW193, CW196, and CW203 (Tencatt *et al*., 2024a, 2025a). Regarding *Brochis*, only two valid species were described from the rio Tapajós basin, *B. bifasciata* (Nijssen, 1972) (= CW135), *B. ornata* (Nijssen & Isbrücker, 1976) (= CW134), although four coded species are known: *Brochis* sp. C143, C152, CW101, CW 192.

In 2023, an expedition to sample tributaries of the rio Tapajós basin in the region of Jacareacanga, Pará State, funded by the renowned Corydoradinae breeder Eric Bodrock (All Oddball Aquatics) and the Greater Pittsburgh Aquarium Society, Inc, resulted in the capture of several Corydoradinae species (Tencatt *et al*., 2025a). Among the captured species are *B. bifasciata*, *Corydoras caramater* Tencatt, Couto, Santos & Sousa, 2024 (= CW83), *Gastrodermus* cf. *pygmaeus* (Knaack, 1966), the recently described *H. noxium* and *H. tenebrosum*, plus nine morphotypes recognized by the aquarium trades under the codes C151, C152, CW66, CW101, CW102, CW127, CW174, CW176 and CW193. As mentioned in Tencatt *et al.* (2024a), *C. caramater* specimens from the rio Tapajós basin are often found in syntopy with two undescribed mimetic species, *Brochis* sp. CW101 and *Hoplisoma* sp. CW102 *sensu* Dias *et al.* (2025). The three species share a peculiar color pattern composed of a dark mask-like blotch transversally crossing the orbit, and lateral body plates only with small, irregular, rounded or vertically elongated dark brown or black blotches, with ground color of lateral body plates, especially on dorsolateral series, typically dusky but not forming large, conspicuous black patches. In life, they display an uncommon metallic green and/or blue sheen, which led the local fishermen (the "piabeiros", *i.e*., fishermen specialized in capturing ornamental species) to call them "azulzinhas" (= little blue ones), differing them mainly by their snout shape.

The analysis of specimens of *Brochis* sp. CW101 and *Hoplisoma* sp. CW102 allowed us to confirm them as new to science. Therefore, the aim of this study is to provide a

formal description for both of them. Moreover, an updated identification key to the Corydoradinae species from the rio Tapajós basin is provided. Also, the possible positive adaptive value of their color pattern is discussed.

MATERIAL AND METHODS

The generic placement of the two new species was based on the morphological diagnoses compiled in Dias *et al.* (2025). Measurements were obtained using digital calipers to the nearest tenth of millimeter. Morphometric and meristic data were taken following Tencatt *et al.* (2022b) and Reis (1997), respectively. Morphometrics are reported as percent of standard length (SL) or head length (HL). Regarding the orientation of the serrations on the posterior margins of the dorsal and pectoral spines, terminology is according to Ballen, de Pinna (2021). For the osteological analysis, some specimens were cleared and stained (c&s) according to the protocol of Taylor, Van Dyke (1985). Due to fading of bone staining, some paratypes were re-stained in a solution of 75% ethyl alcohol and alizarin red S (Springer, Johnson, 2000) after dissection. Osteological terminology was based on Reis (1998), except for the use of parieto-supraoccipital instead of supraoccipital (Arratia, Gayet, 1995), pterotic-extrascapular instead of pterotic-supracleithrum (Slobodian, Pastana, 2018), and scapulocoracoid instead of coracoid (Lundberg, 1970). Nomenclature of the latero-sensory canals and preopercular pores are according to Schaefer, Aquino (2000) and Schaefer (1988), respectively. The supra-preopercle *sensu* Huysentruyt, Adriaens (2005) was treated here as a part of the hyomandibula according to Vera-Alcaraz (2013). The terminology regarding mesethmoid and snout morphology follows Tencatt *et al.* (2025a), including their reinterpretation of the characters-states of character 2 in Vera-Alcaraz (2013:53). Mouth-related structures are according to Tencatt *et al.* (2026), with the terminology of barbels following Britto, Lima (2003). The opening of the axillary gland was considered according to Kiehl *et al.* (2006). The small cartilage between the upper principal and procurrent caudal-fin rays was presumed to be the opisthural cartilage as presented in Monod (1968) and McDowall (1999). To determine the development degree of the anterior laminar expansion of infraorbital 1 in relation to the nasal capsule, the specimen was positioned to maintain the largest diameter of the nasal capsule horizontally. The width of frontal bone was obtained at the same point as the least interorbital width. Vertebral counts include only free centra (*i.e.*, post-Weberian complex), with the compound caudal centrum (preural 1+ ural 1) counted as a single element. The relative size of dorsal-, pectoral-, pelvic- and anal-fin rays is analyzed qualitatively, comparing each ray in erected position (fin fully abducted), with the largest fin element as the main reference. The last two dorsal-fin rays were counted as distinct elements. Pharyngeal teeth were counted on both sides of the branchial arches. In the photos illustrating c&s specimens, the apparent size of some structures may eventually be altered by the perspective from which the photo was taken (*e.g.*, it was not possible to perfectly align the mesethmoid in the horizontal plane in all photographed specimens, especially in dorsal view).

In the description, numbers in parentheses represent the total number of specimens with those counts. Numbers with an asterisk refer to the counts of the holotype. In

the color pattern descriptions, the longitudinal markings on the body are referred to as stripes, whereas the transversal markings on the head and trunk are referred to as bars; the transversal markings on fins are referred to as bands. Institutional abbreviations follow Sabaj (2026). Political geography data of the type material is presented in the following order: country, state and municipality. The conservation status of the new species was suggested using the categories and criteria of the International Union for Conservation of Nature guidelines (IUCN Standards and Petitions Subcommittee, 2024).

RESULTS

Brochis bodrocki, new species

urn:lsid:zoobank.org:act:3C27DD39-1B31-4609-85B1-527F346A01CA

(Figs. 1–9; Tab. 1)

Corydoras sp. CW101. —Tencatt *et al*., 2022a:2 (listed as a putative undescribed species). —Tencatt *et al*., 2024a:3 (listed as a putative undescribed species; ecological notes).

Brochis sp. CW101. —Tencatt *et al*., 2025a:4 (listed as a putative undescribed species).

Holotype. MNRJ 56195, 51.0 mm SL, Brazil, Pará, Jacareacanga, rio Pacu, rio Tapajós basin, rio Amazonas basin, approx. 06°06'S 57°35'W, 3–11 Jul 2023, collected by local fishermen.

Paratypes. All from Brazil, Pará, Jacareacanga, rio Tapajós basin, 3–11 Jul 2023, collected by local fisherman, except when noted. INPA 62598, 1, 33.3 mm SL; CPUFMT 8845, 1, 33.5 mm SL, igarapé Limãozinho, 06°03'S 57°48'W, W. M. Ohara, M. Pinheiro & L. F. C. Tencatt. CITL 1733, 2, 32.5–43.1 mm SL; MUBIO 1098, 2, 37.1–40.2 mm SL; INPA 61170, 9, 33.8–47.7 mm SL; NUP 26900, 4, 34.1–47.2 mm SL, same locality as holotype, 3 Mar 2024. CITL 1734, 2 c&s, 41.1–49.4 mm SL; MNRJ 56196, 3, 44.4–52.4 mm SL; MZUSP 131666, 2, 46.8–46.8 mm SL, collected with the holotype.

Diagnosis. *Brochis bodrocki* can be distinguished from its congeners, except for *B. agassizii* (Steindachner, 1876), *B. amandajanea* (Sands, 1995), *B. ambiacus* (Cope, 1872), *B. approuaguensis* (Nijssen & Isbrücker, 1983), *B. bethanae* (Bentley, Grant & Tencatt, 2021), *B. bifasciata*, *B. condiscipulus* (Nijssen & Isbrücker, 1980), *B. crimmeni* (Grant, 1997), *B. cryptica* (Sands, 1995), *B. deweyeri* (Meinken, 1957), *B. imitator* (Nijssen & Isbrücker, 1983), *B. incolicana* (Burgess, 1993), *B. lamberti* (Nijssen & Isbrücker, 1986), *B. ornata*, *B. orphnopterus* (Weitzman & Nijssen, 1970), *B. pulchra* (Isbrücker & Nijssen, 1973), *B. robusta* (Nijssen & Isbrücker, 1980), *B. sychri* (Weitzman, 1960), and *B. virginiae* (Burgess, 1993) by having a large, smoothly arched dark brown or black patch extending from anterior portion of parieto-supraoccipital towards region of interopercle, transversally crossing the orbit and forming the typical mask-like blotch, which can be variably diffuse (*vs.* mask-like blotch absent); it differs from *B. agassizii*, *B. amandajanea*, *B. ambiacus*, *B.*



FIGURE 1 | *Brochis bodrocki*, holotype, MNRJ 56195, 51.0 mm SL, Jacareacanga, Pará, Brazil, rio Pacu, rio Tapajós basin, rio Amazonas basin, approx. 06°06'S 57°35'W, 3–11 Jul 2023, collected by local fishermen.

bifasciata, *B. cryptica*, *B. incolicana*, *B. robusta* and *B. virginiae* by the absence of a large dark brown or black patch around dorsal-fin base (*vs.* presence of a large dark patch at least around anterior portion of the dorsal-fin base); from *B. bethanae*, *B. imitator*, *B. ornata*, *B. orphnopterus*, and *B. pulchra*, plus *B. bifasciata*, *B. incolicana*, and *B. robusta*, by the absence of dark brown or black stripes on flanks (*vs.* presence of at least one dark stripe on flanks); from *B. approuaguensis*, *B. condiscipulus*, and *B. lamberti*, plus *B. agassizii*, *B. ambiacus*, *B. bethanae*, *B. incolicana*, *B. ornata*, *B. orphnopterus*, *B. pulchra*, and *B. robusta*, by having the caudal fin devoid of conspicuous dark markings (*vs.* conspicuous dark markings on caudal fin present); from *B. crimmeni*, *B. deweyeri*, and *B. sychri* by having the lateral

body plates, especially of the dorsolateral series, with conspicuous concentration of dark brown or black chromatophores, with dark blotches on flanks slightly darker than the ground color of plates (*vs.* the dorso- and ventrolateral body plates with pale yellow or beige background coloration, with dark blotches on flanks conspicuously standing out from the ground color of plates in *B. crimmeni* and *B. sychri*; dark markings on flanks, when present, conspicuously standing out from the ground color of plates in *B. deweyeri*). The new species can be further distinguished from *B. deweyeri* and *B. sychri* by having the region around the posterior process of parieto-supraoccipital clearly lighter than its surrounding area, forming a V-shaped pattern in dorsal view (*vs.* absence of such pattern). *Brochis bodrocki* further differs from *B. crimmeni* by having ventral portion of ventrolateral body plates devoid of conspicuous dark brown or black markings; small blotches, if present, diffuse and restricted to the region posterior to anal-fin anterior origin (*vs.* ventral portion of ventrolateral body plates, except for region around pelvic-fin origin in some specimens, covered by conspicuous dark brown or black blotches).

Description. Morphometric data in Tab. 1. Head laterally compressed with acutely convex dorsal profile, roughly triangular in dorsal view. Snout typically long, roughly straight and pointed; intermediate long in some specimens. Head profile convex from tip of snout to anterior nares, ascending nearly straight or slightly convex from this point to dorsal-fin origin; region of mesethmoid and/or frontal fontanel slightly concave in some specimens. Profile nearly straight to slightly convex along dorsal-fin base. Postdorsal-fin body profile slightly concave to adipose-fin spine, concave from this point to caudal-fin base; region between dorsal and preadipose platelets typically

TABLE 1 | Morphometric data of the holotype and 16 paratypes of *Brochis bodrocki*. SD = Standard deviation.

	Holotype	Low–High	Mean±SD
Standard length (mm)	51.0	32.5–52.4	
Percent of standard length			
Depth of body	39.6	37.4–42.6	40.1±1.2
Predorsal distance	54.7	52.4–55.9	54.6±0.9
Prepelvic distance	49.2	47.6–52.3	50.0±1.2
Preanal distance	83.5	81.2–84.8	83.1±0.9
Preadipose distance	85.5	85.1–88.7	86.2±1.0
Length of dorsal spine	24.9	22.5–27.3	24.8±1.1
Length of pectoral spine	21.6	18.6–26.1	23.4±2.1
Length of adipose-fin spine	8.4	7.9–9.8	9.0±0.6
Depth of caudal peduncle	13.1	12.8–15.7	14.5±0.9
Length of dorsal-fin base	19.6	18.2–20.9	19.5±0.8
Dorsal to adipose distance	15.7	13.7–18.2	16.2±1.2
Maximum cleithral width	25.9	23.3–26.7	25.3±0.8
Length of outer mental barbel	17.8	15.4–23.8	19.6±2.1
Head length	47.8	45.7–49.1	47.6±0.8
Percent of head length			
Head depth	79.1	75.5–82.0	78.6±1.6
Least interorbital distance	29.5	29.5–32.6	31.0±0.8
Horizontal orbit diameter	19.3	18.7–22.6	21.0±1.2
Snout length	46.3	42.4–47.4	44.8±1.5
Least internarial distance	14.3	14.0–16.1	15.1±0.8

nearly straight. Ventral profile of body nearly straight to slightly convex from isthmus to pectoral girdle, and slightly convex from this point until pelvic girdle. Profile nearly straight to slightly convex from pelvic girdle to base of first anal-fin ray, ascending concave until caudal-fin base. Body roughly elliptical in cross section at pectoral girdle, gradually becoming more compressed toward caudal fin. Highest body depth at vertical through dorsal-fin origin.

Eye rounded, located dorsolaterally on head. Orbit delimited anteriorly by lateral ethmoid, anterodorsally by frontal, posterodorsally by sphenotic, posteroventrally by infraorbital 2, and anteroventrally by infraorbital 1 (Fig. 2A). Anterior and posterior nares close to each other, separated only by flap of skin. Anterior naris tubular; posterior naris close to anterodorsal margin of orbit, separated from it by distance similar to or about twice naris diameter. Mouth small, subterminal, width similar to bony orbit diameter; skin fold extending from region just dorsolateral to mouth towards anteroventral portion of preopercle, forming lateral fold at anteroventral portion of snout; lateral fold entirely fleshy, short, not reaching anterior margin of orbit in a vertical, its posterior portion expanded laterally, forming ventrolateral groove; area at mouth corner, just ventral to anterior portion of lateral fold, with small, wrinkle of skin; posteroventral margin of maxillary bulb typically smooth, slightly projected ventrally, some specimens with conspicuous, rounded fleshy expansion; dorsal portion of maxillary bulb typically with small, roughly triangular skin flap; posterolateral margin of lower lip poorly to moderately developed, roughly triangular to slightly rounded. Outer mental barbel typically well developed, reaching to or slightly surpassing anteroventral limit of gill opening; moderately developed, not reaching anteroventral limit of gill opening in some specimens, apparently due to ongoing regeneration. Maxillary barbel typically similar in size or slightly longer than outer mental barbel; slightly shorter than outer mental barbel in some specimens, apparently due to ongoing regeneration; small, roughly rounded to triangular mesial skin fold from posteroventral portion of upper lip to anteroventral portion of barbel. Inner mental barbel fleshy, base of each counterpart slightly separated from each other; mesial notch typically deep. Small rounded papillae covering entire surface of all barbels, upper and lower lips, snout and isthmus.

Mesethmoid long in size, its length slightly larger than frontal length; anterior tip roughly straight or slightly inclined upwards in lateral view, relatively short, slightly smaller than 50% of bone length; posterior margin narrow, its width clearly smaller than maximum width of posterior portion of bone; base conspicuously short to short, lateral posterodorsal expansion with wide roughly triangular or trapezoid external projection, emerging just anterior to or relatively close to distal point of suture with frontal, respectively; external projection conspicuously short, its distal tip reaching mesial edge of nasal bone, to short, its distal tip not reaching lateral edge of nasal bone; posterodorsal portion covered by thick layer of skin; posterior ventrolateral expansion clearly visible in dorsal view, emerging on middle portion of mesethmoid, further anteriorly to external projection of lateral posterodorsal expansion (Figs. 2B, 3A). Upper jaw with tooth-like structures on ventral margin, especially on paratype CITL 1734 (41.1 mm SL); lower jaw edentulous; premaxilla overall funnel-like shaped, with anteroventral surface roughly triangular to square in frontal view; anteroventral margin irregular; posterodorsal portion with conspicuous pointed process, mesially set in frontal view (Fig. 4A); maxilla elongated, relatively slender and roughly hatchet shaped in

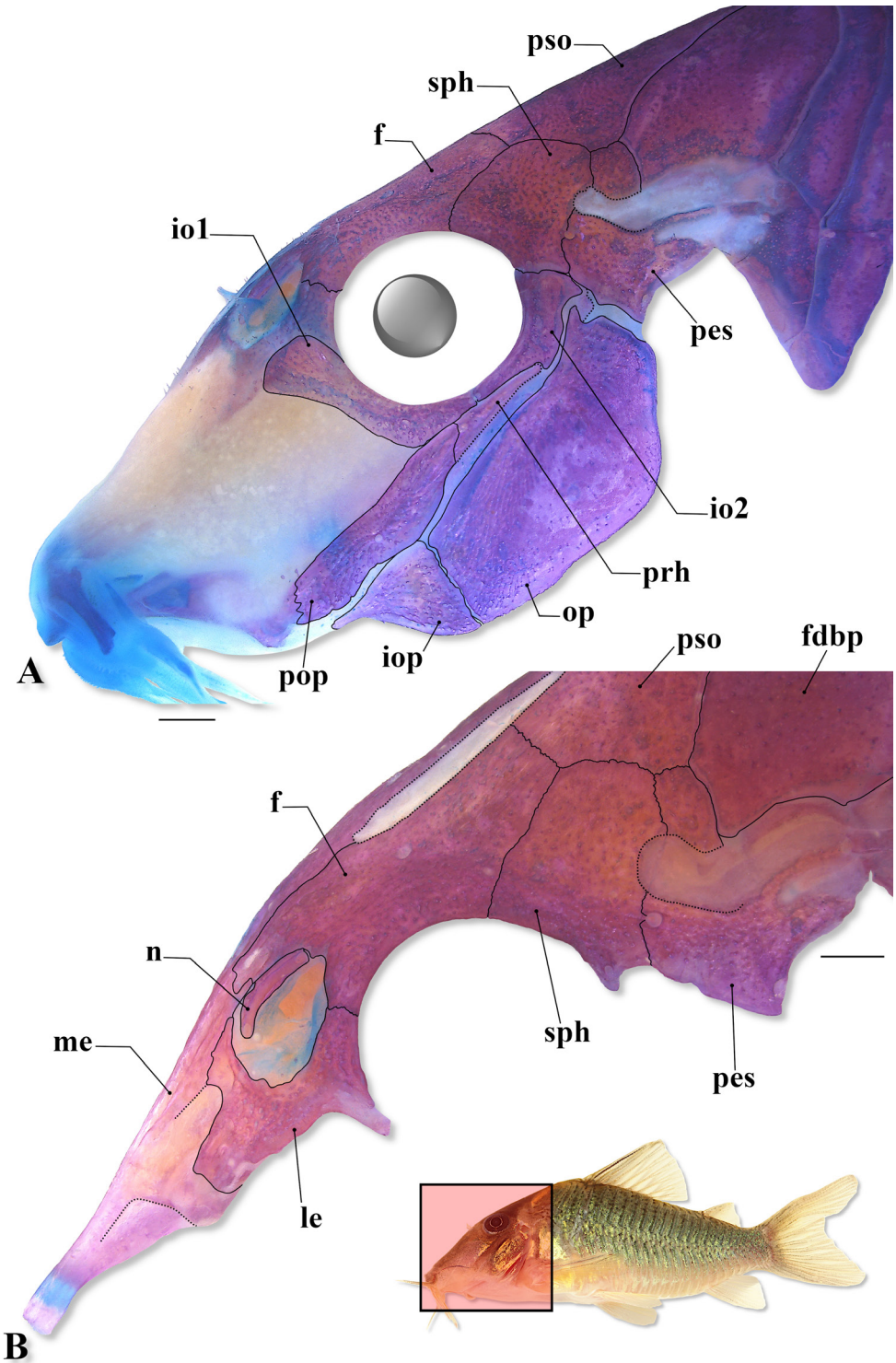

FIGURE 2 | Head osteological pattern in a c&s paratype of *Brochis bodrocki* (CITL 1734, 49.4 mm SL), showing (**A**) general morphology in lateral view, and (**B**) the anterior portion of neurocranium in lateral view. Abbreviations: f: frontal, fdbp: first dorsolateral body plate, io1–2: infraorbital 1 and 2, iop: interopercle, le: lateral ethmoid, n: nasal, me: mesethmoid, op: opercle, pes: pterotic-extrascapular, pop: preopercle, prh: posterodorsal ridge of hyomandibula, pso: parieto-supraoccipital, sph: sphenotic. Area where the illustrated bones are located in fish's body marked in red in the miniature photo in life of the holotype of the new species in lateral view. Scale bars = 1 mm.

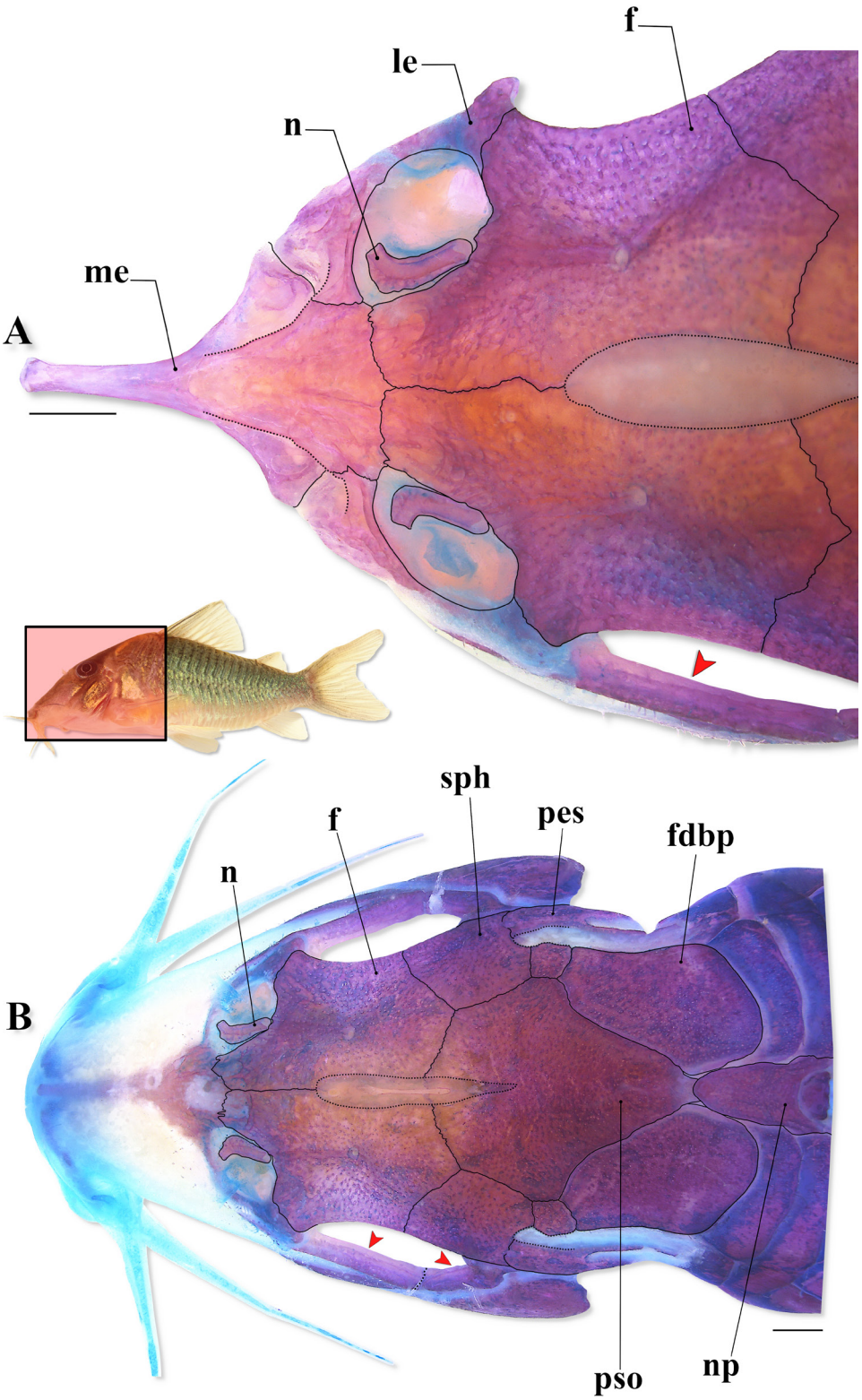

FIGURE 3 | Cranial osteology in a c&s paratype of *Brochis bodrocki* (CITL 1734, 49.4 mm SL), showing (**A**) the anterior portion of neurocranium, and (**B**) the predorsal portion of body, both in dorsal view. Abbreviations: f: frontal, fdbp: first dorsolateral body plate, le: lateral ethmoid, me: mesethmoid, n: nasal, np: nuchal plate, pes: pterotic-extrascapular, pso: parieto-supraoccipital, sph: sphenotic. Red arrows indicate inner laminar expansion of both infraorbitals. Area where the illustrated bones are located in fish's body marked in red in the miniature photo in life of the holotype of the new species in lateral view. Scale bars = 1 mm.

frontal view, its proximal half with roughly triangular to trapezoid laminar process on posterolateral portion (Fig. 4A); dentary relatively slender, with roughly trapezoid to triangular expansion on its anteroventral portion, in ventrolateral perspective, smoothly bent anteriorly, directed mesially; roughly triangular process on its posterodorsal portion, conspicuously bent posteriorly; angulo-articular relatively deep posteriorly, with roughly triangular to trapezoid dorsal laminar expansion, slightly bent posteriorly; posteroventral portion with roughly triangular process, in lateral view, bent posteriorly (Fig. 4B). Palatine longitudinally elongated, moderate-sized, with roughly triangular to rounded or trapezoid dorsolateral laminar expansion on its posterior portion, articulating with lateroventral expansion of posterior portion of mesethmoid; posterolateral process well developed, extending posteriorly in parallel to dorsal margin of anterior laminar expansion of metapterygoid (Fig. 4C).

Nasal capsule delimited posteriorly and dorsally by frontal, anterodorsally by mesethmoid, and anteriorly, ventrally and posteriorly by lateral ethmoid (Figs. 2A, 3A). Nasal slender, laterally curved, inner margin typically with poorly-developed laminar expansion, contacting only frontal; outer margin with strongly reduced laminar expansion (Figs. 2B, 3). Lateral ethmoid moderately deep in lateral view, entirely covered by thick skin layer; posterior portion with relatively wide roughly triangular posteroventral expansion, and relatively long and wide roughly trapezoid posterodorsal expansion; distinct curved posteriorly or roughly trapezoid anterodorsal expansion, its posterodorsal portion relatively distant from nasal, and anterodorsal margin contacting external projection of lateral posterodorsal expansion of mesethmoid; anteroventral expansion strongly well developed, conspicuously expanded anteroventrally, contacting ventrolateral expansion of posterior portion of mesethmoid by means of large cartilage block (Fig. 2B). Frontal elongated, narrow, width less than half of entire length; anterior projection partially covered by thick layer of skin; anterolateral process roughly trapezoid, relatively wide in lateral view (Fig. 3). Frontal fontanel large, slender, and somewhat ellipsoid; posterior tip extension clearly surpassing anterior margin of parieto-supraoccipital (Figs. 2B, 3). Sphenotic somewhat trapezoid, contacting parieto-supraoccipital dorsally, pterotic-extrascapular posteriorly, second infraorbital posteroventrally and frontal anteriorly (Fig. 2A). Pterotic-extrascapular roughly pipe-shaped, with posteriormost portion contacting first lateral-line ossicle, posteroventral margin contacting cleithrum, and anteroventral margin contacting opercle and infraorbital 2; posterior expansion almost entirely covering lateral opening of swimbladder capsule, leaving slender area on its dorsal margin covered only by thick layer of skin (Fig. 2). Parieto-supraoccipital wide, posterior process long, contacting nuchal plate; region of contact between posterior process and nuchal plate covered by thick layer of skin (Fig. 3B).

Two laminar infraorbitals with minute odontodes. Infraorbital 1 large, ventral laminar expansion typically ranging from poorly to moderately developed (Figs. 2A, 4D); ventral laminar expansion variably well developed; anterior portion typically with conspicuously well-developed laminar expansion, reaching to or slightly surpassing anterior margin of nasal capsule; inner laminar expansion strongly reduced (Figs. 2A, 3, 4D). Infraorbital 2 small, widened dorsally, with posterior laminar expansion moderately to well developed (Figs. 2A, 4D); posteroventral margin contacting posterodorsal ridge of hyomandibula, posterior margin typically close but not in direct contact

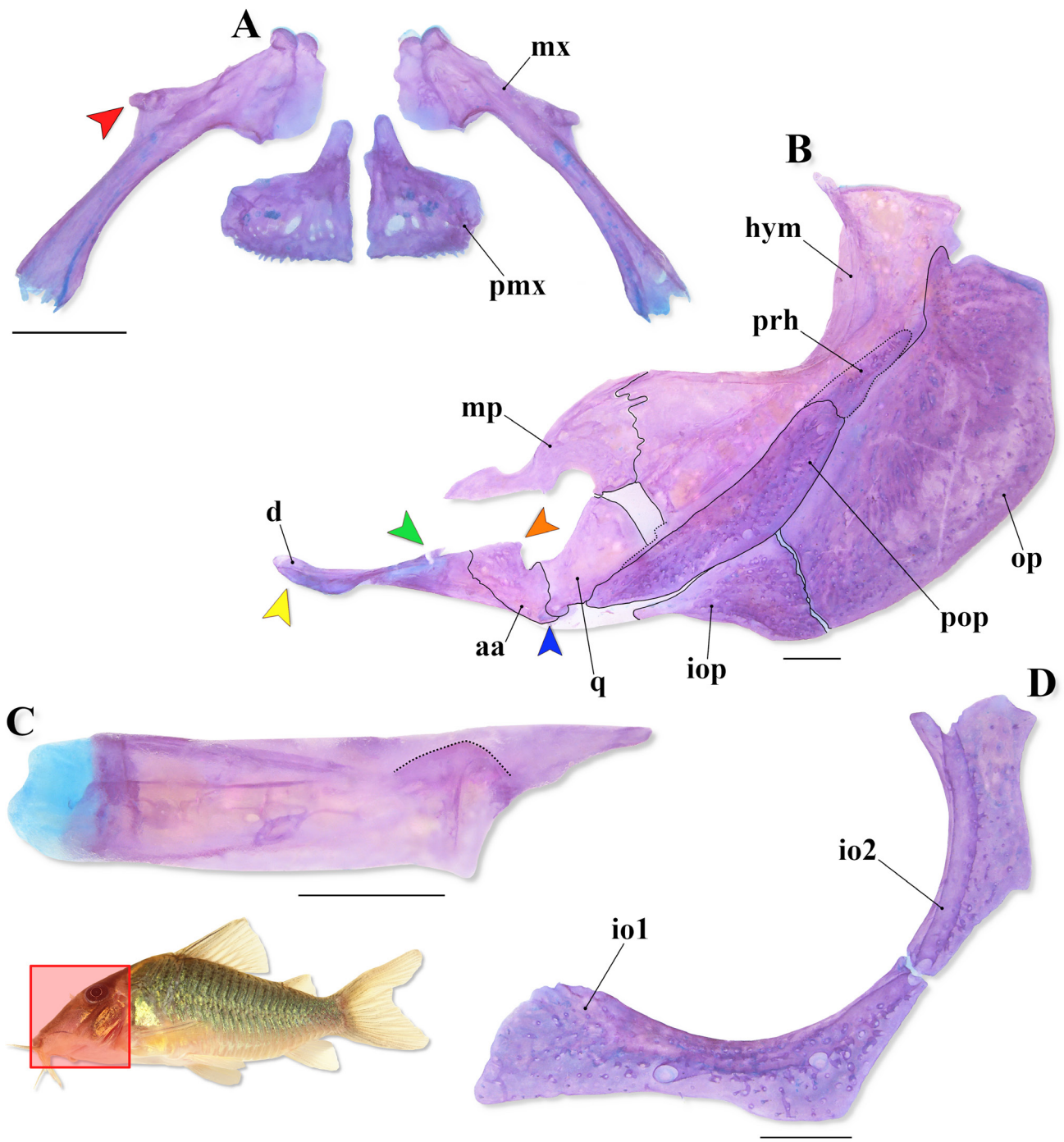

FIGURE 4 | Cranial osteology in a c&s paratype of *Brochis bodrocki* (CITL 1734, 41.1 mm SL), showing (**A**) the upper jaw in frontal view (= dorsal view considering everted mouth), (**B**) the suspensorium plus operculum in lateral view, (**C**) the palatine in dorsal view, and (**D**) the infraorbital series in lateral view. Abbreviations: aa: angulo-articular, d: dentary, hym: hyomandibula, io1–2: infraorbital 1 and 2, iop: interopercle, mp: metapterygoid, mx: maxilla, op: opercle, pmx: premaxilla, pop: preopercle, prh: posterodorsal ridge of hyomandibula, q: quadrate. Red arrow indicates laminar process on posterolateral portion of maxilla; yellow and green arrows indicate anteroventral expansion (not visible in this perspective) and posterodorsal process of dentary, respectively; orange and blue arrows indicate dorsal laminar expansion and posteroventral process of angulo-articular, respectively. Dotted line in (**C**) outlining dorsolateral longitudinal laminar expansion of palatine. Area where the illustrated bones are located in fish's body marked in red in the miniature photo in life of the holotype of the new species in lateral view. Scale bars = 1 mm.

with opercle, or in direct contact with opercle, and posterodorsal edge contacting sphenotic and pterotic-extrascapular (Fig. 2A); posterodorsal portion typically with roughly triangular expansion, and middle portion with moderately-developed roughly triangular expansion, bent downwards, with tip just above dorsal edge of posterodorsal ridge of hyomandibula (Figs. 2A, 4D); inner laminar expansion strongly reduced (Figs. 2A, 3B, 4D). Posterodorsal ridge of hyomandibula close to its articulation with opercle conspicuously slender, exposed, and bearing small odontodes (Figs. 2A, 4B). Dorsal ridge of hyomandibula between pterotic-extrascapular and opercle typically covered by thick layer of skin. Interopercle entirely or partially covered by thick layer of skin; posterior portion variably exposed and bearing odontodes; subtriangular, anterior projection moderately to well developed (Figs. 2A, 4B). Preopercle elongated, relatively slender; minute odontodes on external surface (Figs. 2A, 4B). Opercle dorsoventrally elongated, with width slightly smaller than half of its entire length; free margin convex, without serrations and covered by small odontodes (Figs. 2A, 4B).

Four branchiostegal rays decreasing in size posteriorly. Hypobranchial 1 deep; hypobranchial 2 somewhat triangular, tip ossified and directed towards anterior portion, posterior margin cartilaginous; ossified portion well developed, its size about twice cartilaginous portion. Five ceratobranchials with expansions increasing posteriorly; ceratobranchial 1 with strongly reduced to small process on anterior margin of mesial portion; ceratobranchial 3 typically notched on postero-lateral margin; ceratobranchial 5 toothed on posterodorsal surface, with 34 to 38(2) teeth aligned in one row. Four epibranchials with similar size; epibranchial 2 slightly larger than others, with small, roughly trapezoid or pointed process on laminar expansion of posterior margin, typically with notch just ventral to process; epibranchial 3 with roughly triangular to trapezoid uncinate process on laminar expansion of posterior margin, bent mesially. Two wide pharyngobranchials (3 and 4); pharyngobranchial 3 with roughly triangular, rounded or trapezoid laminar expansion on posterior margin; laminar expansion variably notched. Upper tooth plate roughly oval, 37 to 38(1) teeth aligned in two rows on posteroventral surface; rows closely aligned; paratype CITL 1734, 49.4 mm SL, apparently with malformation in tooth plate.

Lateral-line canal reaching cephalic laterosensory system through pterotic-extrascapular, branching twice before reaching sphenotic: pterotic branch, with single pore, preoperculomandibular branch conspicuously reduced, with single pore opening at or close to postotic main canal; postotic main canal widens just posterior to pterotic branch. Sensory canal continuing through pterotic-extrascapular, reaching sphenotic as temporal canal, which splits into two branches: one branch giving rise to infraorbital canal, other branch connecting to frontal through supraorbital canal, both with single pore. Supraorbital canal branched, running through nasal bone. Epiphyseal branch conspicuously reduced; pore opening close to supraorbital main canal, directed towards frontal fontanel. Nasal canal with three openings, first on posterior edge, second on posterolateral portion, typically fused with first pore, and third on anterior edge. Infraorbital canal running through entire infraorbital 2, extending to infraorbital 1 and typically opening into two pores; variably into single pore. Preoperculomandibular branch giving rise to preoperculo-mandibular canal, which runs through almost entire preopercle with three openings, leading to pores 3, 4, and 5, respectively; pore 3 variably opening at posterodorsal ridge of hyomandibula.

Dorsal fin subtriangular, typically located just posterior to second dorsolateral body plate. Dorsal-fin rays II,8(17), with first branched ray typically as longest fin element; branched rays typically decreasing in size posteriorly, with first and second, and variably third, branched rays slightly longer than ossified portion of dorsal-fin spine, remaining rays with similar size or shorter than spine; second or third branched ray variably as longest fin element; second and third branched rays slightly longer than first branched ray in some specimens; third branched ray shorter or similar in size to ossified portion of spine in some specimens; branched rays on middle portion of dorsal fin smaller than adjacent rays in some specimens, forming notch on dorsal-fin posterior margin; first and second branched rays variably clearly more elongated than spine, especially in smaller specimens (up to about 40.0 mm SL); posterior margin of dorsal-fin spine with 15 to 23 strongly reduced to moderately-developed laminar serrations; most serrations retrorse, with some serrations variably antrorse or perpendicularly directed (relative to main axis of spine), especially on proximal portion of spine; serrations absent close to origin of spine; small odontodes on anterior and lateral surfaces of spine (Fig. 5A). Nuchal plate well developed, almost entirely exposed, with minute odontodes. Spinelet short; spine typically moderately developed, with adpressed distal tip slightly surpassing dorsal-fin terminus. Pectoral fin roughly triangular, its origin just posterior to gill opening. Pectoral-fin I,7(1), I,8(1), I,8,i(1), I,9*(9), I,9,i(2), I,10(3), with first branched ray typically as longest fin element; branched rays typically decreasing in size posteriorly, with first and second branched rays slightly longer than ossified portion of pectoral-fin spine, remaining rays with similar size or shorter than spine; first and second branched rays with similar size in some specimens; second branched ray variably similar in size to ossified portion of spine; third branched ray variably longer than ossified portion of spine; posterior margin of pectoral spine with 16 to 22 strongly reduced to moderately-developed laminar serrations along almost its entire length, absent close to origin of spine; most serrations retrorse, some serrations variably antrorse or perpendicularly directed (relative to main axis of spine), especially on proximal portion of spine; small odontodes on anterior, dorsal and ventral surfaces of spine (Fig. 5B). Anteroventral portion of cleithrum and anterolateral portion of scapulocoracoid exposed; posterolateral portion of scapulocoracoid moderately developed, exposed, with anterior portion typically conspicuously expanded anteriorly, contacting anteroventral portion of cleithrum; posterolateral portion of scapulocoracoid variably with anterior portion less expanded anteriorly, not in contact with anteroventral portion of cleithrum, especially in smaller specimens (up to about 40.0 mm SL); exposed areas bearing small odontodes. Opening of axillary gland located just posterior to pectoral-fin spine base.

Pelvic fin oblong, typically located just below second ventrolateral body plate, and at vertical through first or second dorsal-fin branched ray. Pelvic-fin rays i,5* (17); second branched ray typically as longest fin element, with rays decreasing in size towards both anterior and posterior margins of fin; second branched ray variably as long as third branched ray; unbranched ray or last branched ray as shorter fin element. Anterior internal process of basipterygium well developed and moderately laterally expanded, with obliquely placed dorsal lamina, smoothly converging mesially towards anterior edge of process, with counterparts not contacting each other anteriorly, roughly triangular in lateral view, curved posteriorly, and variably bent mesially; ventral laminar expansion obliquely placed, converging mesially towards anterior edge of process, with



FIGURE 5 | Lateral view of (**A**) the dorsal-fin spine and dorsal view of (**B**) the right pectoral-fin spine in a c&s paratype of *Brochis bodrocki* (CITL 1734, 49.4 mm SL), showing their serration patterns. Area where the illustrated bones are located in fish's body marked in red in the miniature photo in life of the holotype of the new species in lateral view. Scale bars = 1 mm.

counterparts contacting each other anteriorly, clearly less developed than dorsal lamina; anterior external process laminar, moderately developed and slightly to moderately expanded posteriorly, variably notched on anterior margin; dorsal ischiac process well developed, typically with irregular lateral margin, anterior laminar expansion conspicuously expanded anteriorly, roughly trapezoid or irregular, and posterior laminar expansion slightly to moderately expanded posteriorly, roughly triangular or irregular; ventral ischiac process clearly smaller than dorsal process, roughly triangular, bent anteriorly (Fig. 6). Adipose fin roughly triangular, separated from base of last dorsal-fin ray by five to six dorsolateral body plates. Anal fin subtriangular, located just posterior to 13th or 14th ventrolateral body plates, and at vertical through adipose-fin spine base or region of adipose-fin membrane. Anal-fin rays ii,6*(17); third ray typically as longest fin element, with rays decreasing in size towards both anterior and posterior margins of fin; fourth ray variably similar in size or longer than third ray; last ray typically as shorter fin element, variably similar in size to first ray. Caudal fin bilobed, typically with dorsal lobe slightly larger than ventral lobe, or dorsal and ventral lobes similar in size;

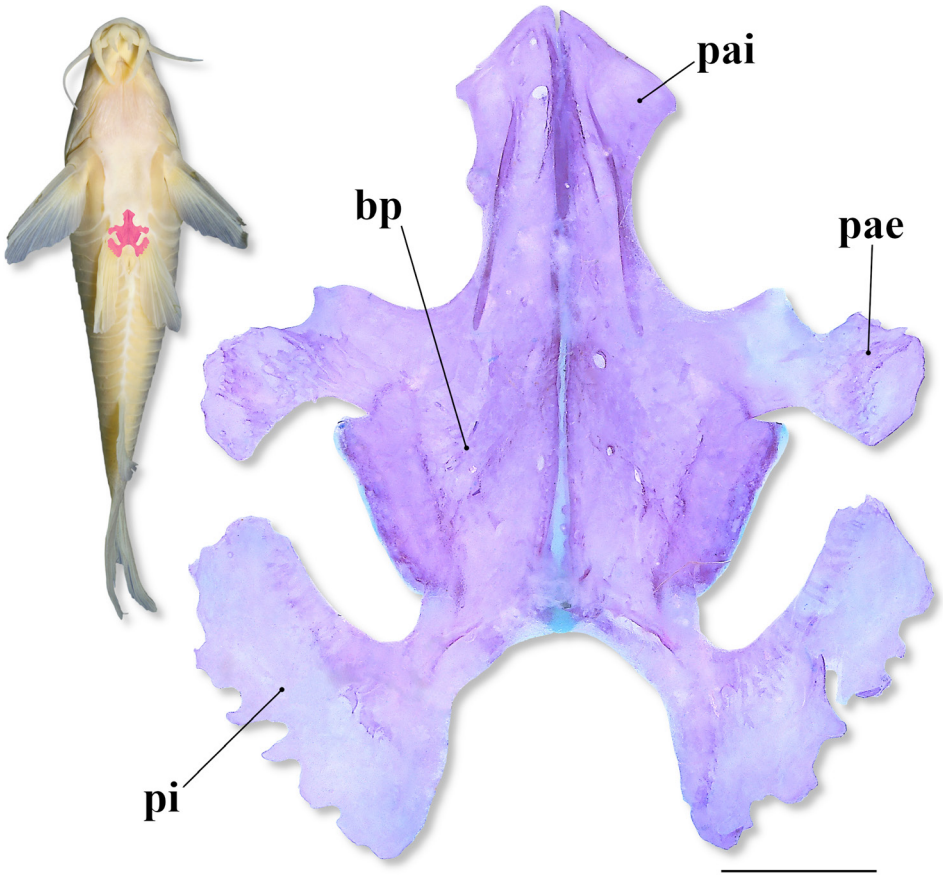

FIGURE 6 | Pelvic girdle in a c&s paratype of *Brochis bodrocki* (CITL 1734, 49.4 mm SL). Abbreviations: bp: basipterygium, pae: anterior external process, pai: anterior internal process, pi: dorsal ischiac process. Area where the illustrated bones are located in fish's body marked in red in the miniature photo of the preserved holotype of the new species in ventral view. Scale bar = 1 mm.

some specimens undergoing caudal regeneration with dorsal lobe smaller than ventral lobe. Caudal-fin rays i,11,i*(1), i,12,i(16), with generally five or six dorsal and ventral procurrent rays increasing in size posteriorly; small cartilage between upper principal and procurrent caudal-fin rays (presumably opisthural cartilage) observed in paratype CITL 1734, 41.1 mm SL (Fig. 7).

Three or four laterosensory canals on trunk; first ossicle tubular, second ossicle laminar, both bearing small odontodes; third and fourth, if present, encased in third and fourth dorsolateral body plates, respectively. Body plates with minute odontodes scattered over exposed area, with conspicuous line of odontodes confined to posterior margins. Dorsolateral body plates 23(1), 24*(11), 25(5); ventrolateral body plates 21(5), 22*(10), 23(2). Dorsolateral body plates along dorsal-fin base 6*(6), 7(11); dorsolateral body plates between adipose- and caudal-fin 7(2), 8*(14), 9(1). Preadipose platelets 1(1), 2*(12), 3(4). Ventral surface of trunk between posteroventral margin of cleithrum and pelvic-fin origin typically laterally delimited only by first ventrolateral body plate; ventral portion of first ventrolateral body plate ranging from slightly to moderately expanded anteriorly. Small platelets covering base of caudal-fin rays; small platelets

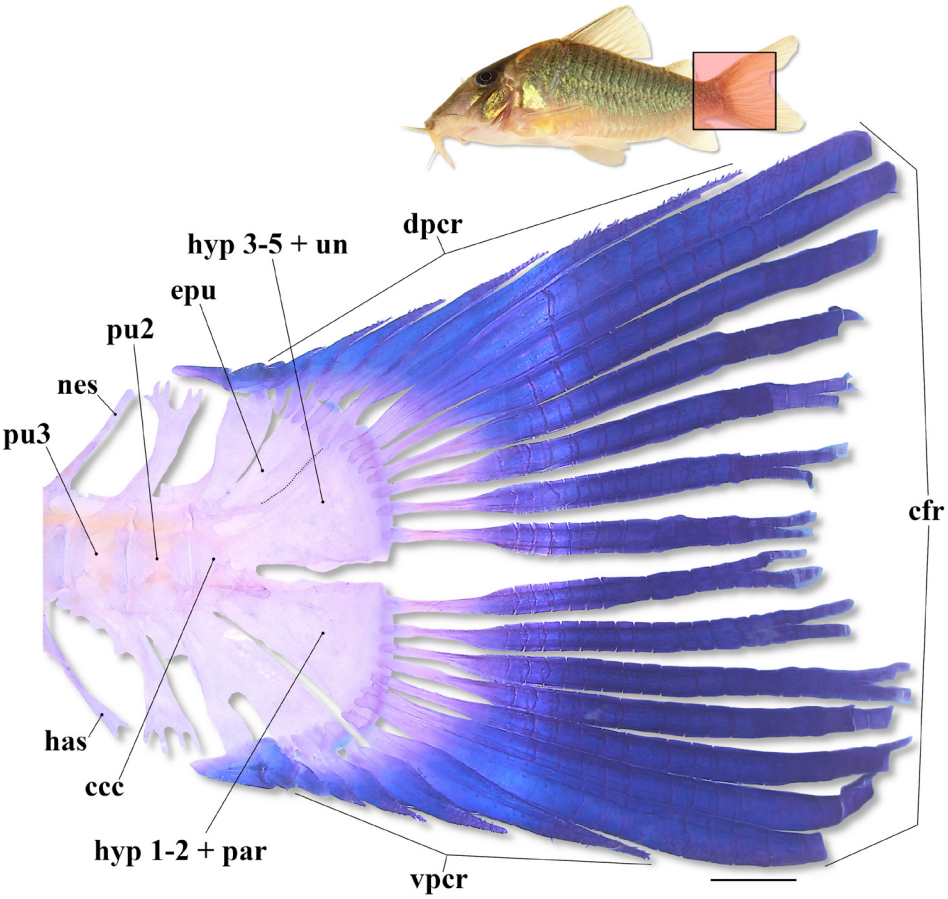

FIGURE 7 | General morphology of caudal skeleton in a c&s paratype of *Brochis bodrocki* (CITL 1734, 49.4 mm SL). Abbreviations: ccc: compound caudal centrum, cfr: caudal-fin principal rays, dpcr: dorsal procurrent rays, epu: epural, has: haemal spine, hyp 1–5: hypurals 1 to 5, nes: neural spine, par: parhypural, pu 2–3: preural centra 2 to 3, un: uroneural, vpcr: ventral procurrent rays. Area where the illustrated bones are located in fish's body marked in red in the miniature photo in life of the holotype of the new species. Scale bar = 1 mm.

disposed dorsally and ventrally between junctions of lateral plates on posterior portion of caudal peduncle. Region around nasal capsule, above lateral ethmoid, posterior portion of dorsal surface of mesethmoid, and posteroventral portion of lateral surface of snout with small-sized platelets bearing odontodes. Belly typically covered by numerous small- to relatively large-sized platelets; smaller c&s paratype (CITL 1734, 41.1 mm SL) with fewer small-sized platelets bearing odontodes, more concentrated mesially; platelets variably closely-spaced, but not forming typical mosaic-like pattern; platelets irregular in shape and bearing odontodes (Fig. 8).

Vertebral count 22(2); ribs 7(2); first pair conspicuously large, its middle portion closely connected to first ventrolateral body plate; its tip connected to anterior external process of basipterygium. Parapophysis of complex vertebra moderately or well developed.

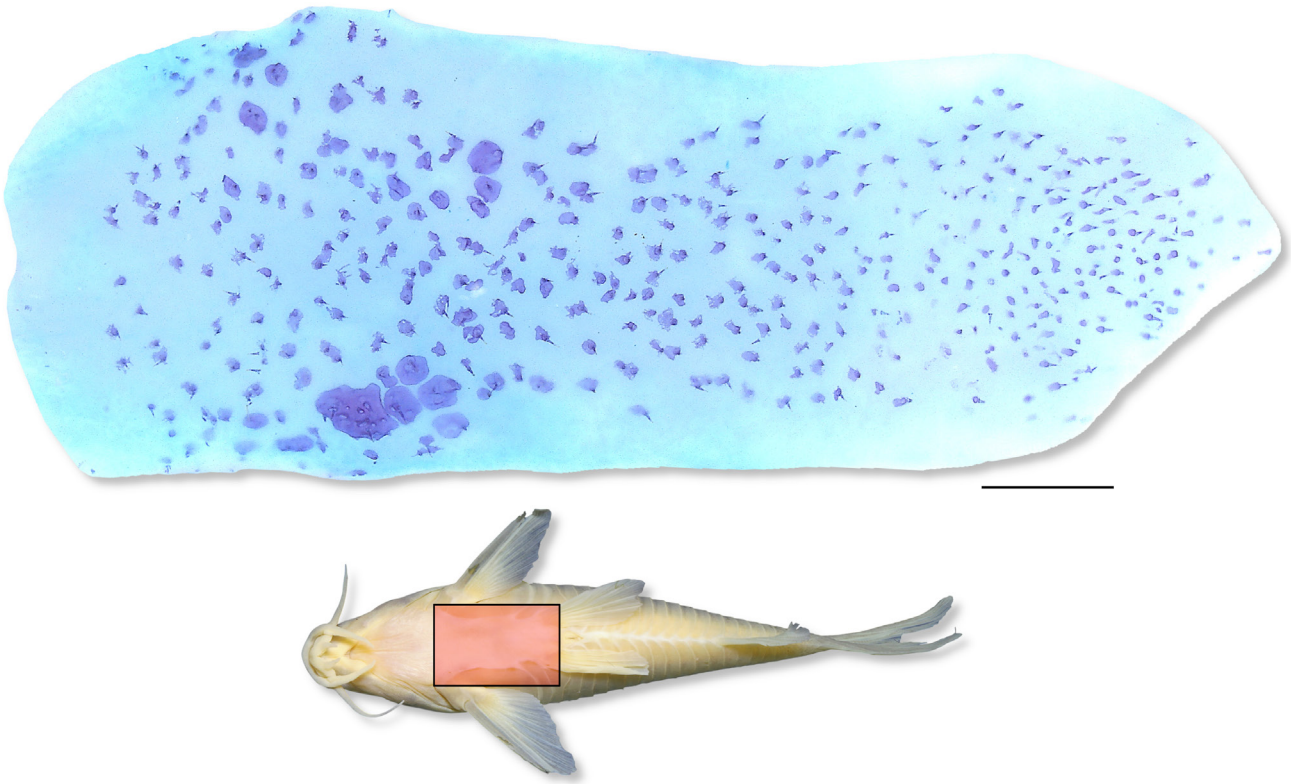

FIGURE 8 | Ventral surface of trunk in a c&s paratype of *Brochis bodrocki* (CITL 1734, 49.4 mm SL), showing the small to relatively large, irregular platelets on the belly. Area where the illustrated structures are located in fish's body marked in red in the miniature photo of the preserved holotype of the new species in ventral view. Scale bar = 1 mm.

Coloration in alcohol. Overall color pattern of body in Fig. 1. Ground color of body pale- to brownish yellow or beige. Top of head dark brown. Dorsal and lateral surface of head covered by dark brown or black chromatophores, not forming small blotches; lips and barbels with dark brown or black chromatophores, conspicuously more concentrated on upper lip and outer mental barbel; chromatophores on inner mental barbel scarce, apparently absent in some specimens; ventrolateral portion of head variably with dark brown or black chromatophores, with isthmus typically devoid of chromatophores; anterior portion of isthmus with scarce dark brown or black chromatophores in some specimens; large, smoothly arched dark brown or black patch extending from interopercle region to anterior portion of parieto-supraoccipital, transversally crossing orbit, where it meets its counterpart and extends towards posterior process of parieto-supraoccipital, forming typical mask-like blotch with V-shaped pattern in dorsal view; mask-like blotch relatively diffuse, but typically distinct from surrounding areas; some specimens with less evident mask; anterior and middle portions of opercle, especially on its ventral two thirds, with more concentrated dark brown or black chromatophores, forming large, irregular dark patch typically fused with mask-like blotch, posterior margin of bone typically lighter than surrounding areas; region of contact between posterior process of parieto-supraoccipital and first dorsolateral, and nuchal plate clearly lighter than surrounding areas, forming V-shaped pattern in dorsal

view; lateral surface of cleithrum, especially on its middle portion, with conspicuous concentration of dark brown or black chromatophores, variably forming small, rounded to irregular diffuse dark brown or black blotches. Dorsolateral body plates with conspicuous concentration of dark brown or black chromatophores, forming small, irregular, rounded or vertically elongated dark brown or black blotches, slightly darker than ground color of plates; blotches irregularly disposed or roughly vertically aligned. Ventrolateral body plates with conspicuous concentration of dark brown or black chromatophores, forming small, irregular, rounded or vertically elongated dark brown or black blotches, slightly darker than ground color of plates; blotches irregularly disposed or roughly vertically aligned; dark pigmentation gradually reducing towards ventral portion of plates, with blotches typically restricted to dorsal half of plates; region posterior to anal-fin origin with small, diffuse dark blotches on ventral half of plates in some specimens. Posterior margin of body plates typically with dark brown or black chromatophores, forming thin dark lines along border of plates, more evident on dorsal and middle portions of flank. Dorsal, pectoral, pelvic, anal, adipose, and caudal fins with dark brown or black chromatophores, typically not forming dark blotches; chromatophores on dorsal fin variably more concentrated on its anterior portion and/or along its base; dorsal surface of pectoral-fin base on axillary region typically with dark brown or black chromatophores; caudal fin variably with small, diffuse dark blotches, which are typically roughly aligned transversally.

Coloration in life. Similar to color pattern of preserved specimens, but with brighter ground color of body (Fig. 9). Predorsal V-shaped patch typically bright orangish yellow, or golden. Body covered by bluish, or greenish yellow iridescent coloration, especially on region of opercle and cleithrum. Wild-caught and some aquarium specimens typically displaying a green (Fig. 9A) or bluish green metallic sheen on flanks (Figs. 9B–C); some specimens variably lacking such coloration, displaying greyish beige or orangish yellow ground coloration on flanks (Figs. 9D–E). Aquarium specimens variably with dark blotches on lateral surface of head.

Sexual dimorphism. Male specimens of *Brochis bodrocki* present a genital papilla, which is somewhat tubular, a condition well-documented in Corydoradinae (see Britto, 2003; Nijssen, Isbrücker, 1980; Spadella *et al*., 2017).

Geographical distribution. *Brochis bodrocki* is so far known from its type locality, the rio Pacu, and from the igarapé Limãozinho, both tributaries of the rio Tapajós, rio Amazonas basin, Jacareacanga Municipality, Pará State, Brazil (Fig. 10).

Ecological notes. The rio Pacu is relatively large-sized tributary of the right margin of the rio Tapajós (Fig. 11). In the sites where the new species was captured (considering dry season, which tends to be from May to September), the river presents width ranging between 10.0 m and 20.0 m, depth of about 50.0 cm (with deeper sites of about 2.0 m), and slow to moderate water current. The substrate is mostly composed of sand and fine gravel, with stretches accumulating leaf litter and submerged logs/branches. According to the local fishermen, the new species also occur in small tributaries of the rio Pacu (M. A. Pinheiro, 2025, pers. comm.). Although the marginal vegetation is abundant

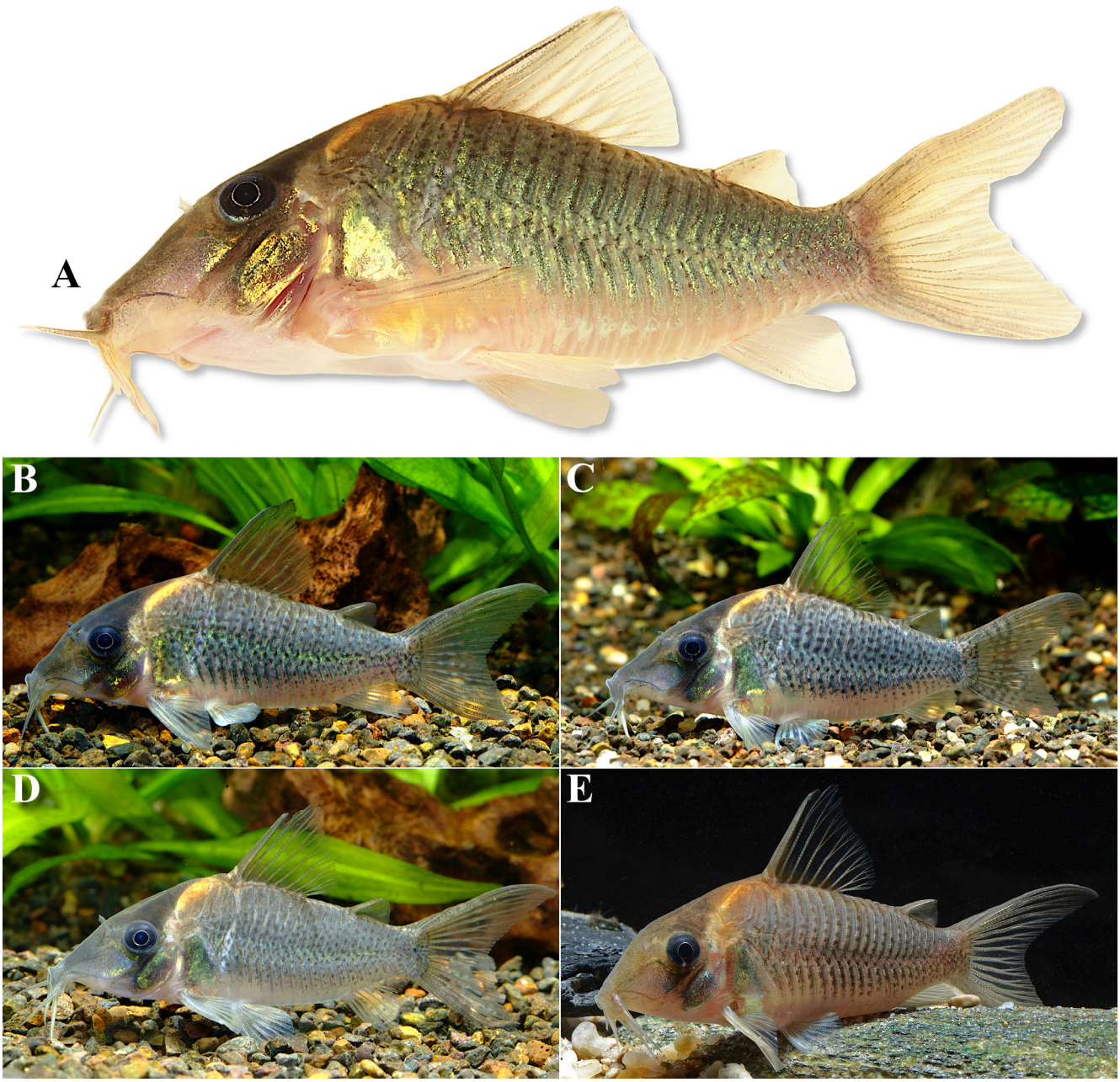

FIGURE 9 | Color pattern in life of *Brochis bodrocki* in lateral view, showing (**A**) the holotype (MNRJ 56195, 51.0 mm SL), and (**B**–**E**) four unpreserved and unmeasured aquarium specimens. Photo (**A**) by WMO, (**B**–**D**) by Wei-Chieh Tseng, and (**E**) Hans Evers.

and the biotope overall well preserved, the water is conspicuously muddy, which is likely to be the result of the intense (illegal) alluvial gold mining activities in the main channel of the rio Pacu. The igarapé Limãozinho is a small-sized tributary of the left margin of the rio Tapajós, characterized by having a crystalline water, width up to about 10.0 m, maximum depth of about 1.0 m, and substrate mostly composed by sand, with faster-flowing waters stretches with submerged vegetation and slower-flowing waters stretches accumulating leaf litter and submerged logs/branches, in the sampled

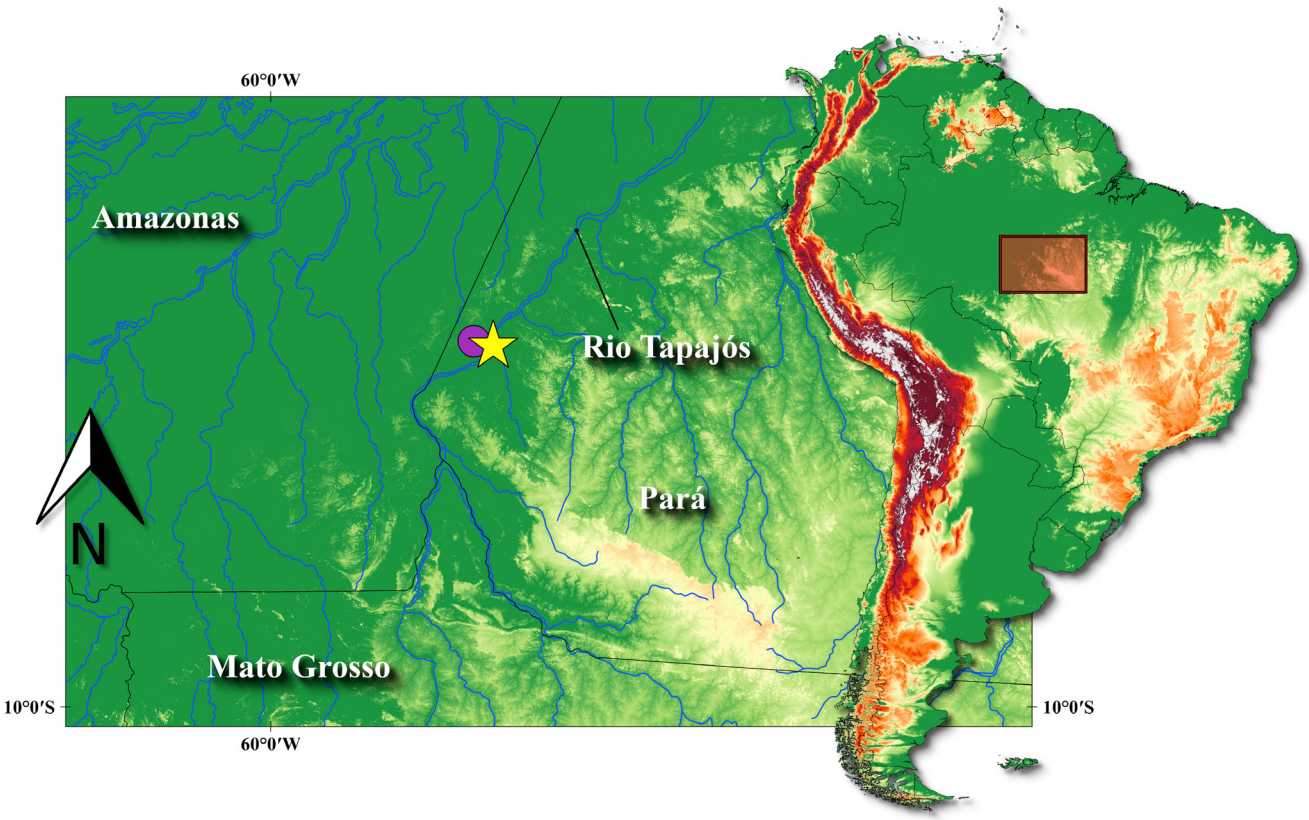

FIGURE 10 | Map showing the known geographic records of *Brochis bodrocki* and *Hoplisoma jujuba* (yellow star: type locality, the rio Pacu; purple circle: igarapé Limãzinho), Pará State, rio Tapajós basin, Brazil.

site. Additionally, stretches with partially exposed submerged roots of marginal trees were also observed. In both localities, the specimens were captured exclusively during the night. In the rio Pacu, *B. bodrocki* occurs in syntopy and shoaling together with *C. caramater* and *H. jujuba* new species, while in the igarapé Limãozinho it co-occurs with both species plus *Hoplisoma* sp. CW193, although not shoaling together with the latter. The new species was observed by LFCT and WMO in the igarapé Limãozinho typically associated with darker substrates, in small numbers (only a single specimen was captured), different from its co-mimic, *H. jujuba*, which was clearly more numerous, though clearly less abundant than *Hoplisoma* sp. CW193. Except for *Hoplisoma* sp. CW193, of which most of the captured individuals were clearly adults, most of the captured specimens of *C. caramater* and both new species were juveniles, with only a few larger specimens of *H. jujuba* at this site. At the rio Pacu, the three co-mimic species, *i.e.*, *C. caramater*, *B. bodrocki* and *H. jujuba* were found in conspicuously higher numbers, mostly adults, with the latter being the most abundant and *B. bodrocki* the less abundant of them.



FIGURE 11 | Rio Pacu, a tributary of the rio Tapajós in the region of Jacareacanga, rio Amazonas drainage, Pará State, Brazil, the type locality of *Brochis bodrocki* and *Hoplisoma jujuba*. Photo by Marcos Pinheiro.

Etymology. *Brochis bodrocki* is named in honor of Eric Bodrock, dear friend and renowned Corydoradinae breeder. Eric, along with the Greater Pittsburgh Aquarium Society, Inc. (USA), made our expedition to Jacareacanga, Pará, possible, which led to the capture of both new species described herein as well as the recently described *Hoplisoma noxium*, *H. tenebrosum*, and several other species of Corydoradinae from the region. A genitive noun.

Conservation status. Currently, the new species is known only from its type locality, the rio Pacu, plus a single additional record, the igarapé Limãozinho, both tributaries of the rio Tapajós basin in Pará State, Brazil. Despite the relatively restricted geographical distribution and the intense alluvial gold mining activities in the region (see Castilhos *et al*., 1998; Crompton *et al*., 2002; Lobo *et al*., 2015; Junior, de Carvalho, 2023), part of the drainage (especially the headwaters) where these water bodies flow is protected by some Conservation Units, especially the Floresta Nacional do Amaná, Floresta Nacional do Urupadi, and also by indigenous territories of the Munduruku ethnic group. In this context, such Conservation Unites likely represent an important refuge for the new species. Therefore, considering the currently available data and according to the International Union for Conservation of Nature (IUCN) categories and criteria (IUCN Standards and Petitions Subcommittee, 2024), *Brochis bodrocki* would be classified as Least Concern (LC).

Hoplisoma jujuba, new species

urn:lsid:zoobank.org:act:C5D6B036-95E3-4DA5-BAC9-C4C445B579E7

(Figs. 12–20; Tab. 2)

Corydoras sp. CW102. —Tencatt *et al*., 2024a:3 (listed as a putative undescribed species; ecological notes).
Hoplisoma sp. CW102. —Tencatt *et al*., 2025a:4 (listed as a putative undescribed species).

Holotype. MNRJ 56197, 44.4 mm SL, Brazil, Pará, Jacareacanga, rio Pacu, rio Tapajós basin, rio Amazonas basin, approx. 06°06'S 57°35'W, 3–11 Jul 2023, collected by local fishermen.

Paratypes. All from Brazil, Pará, Jacareacanga, rio Tapajós basin, 3–11 Jul 2023, collected by local fisherman, except when noted. CITL 1735, 7, 20.0–33.2 mm SL; CPUFMT 8846, 5, 24.7–31.1 mm SL; INPA 62599, 11, 21.6–43.4 mm SL; MUBIO 1099, 7, 19.1–35.5 mm SL; MZUSP 131667, 10, 19.0–35.3 mm SL; NUP 26901, 15, 18.0–38.0 mm SL, igarapé Limãozinho, 06°03'S 57°48'W, W. M. Ohara, M. Pinheiro & L. F. C. Tencatt. MNRJ 56198, 5, 31.1–41.9 mm SL; CITL 1736, 1 c&s, 40.0 mm SL, same locality as holotype, 3 Mar 2024. CITL 1737, 1 c&s, 42.9 mm SL, collected with holotype.

Diagnosis. *Hoplisoma jujuba* can be distinguished from its congeners, except for *H. araguaiaense*, *H. burgessi* (Axelrod, 1987), *H. colossus* (Tencatt, Grant & Bentley, 2023), *H. concolor*, *H. esperanzae*, *H. evelynae*, *H. eversi* (Tencatt & Britto, 2016), *H. granti* (Tencatt,



FIGURE 12 | *Hoplisoma jujuba*, holotype, MNRJ 56197, 44.4 mm SL, Jacareacanga, Pará, Brazil, rio Pacu, rio Tapajós basin, rio Amazonas basin, approx. 06°06'S 57°35'W, 3–11 Jul 2023, collected by local fishermen.

Lima & Britto, 2019), *H. julii*, *H. kanei* (Grant, 1997), *H. noxium*, *H. melanistium* (Regan, 1912), *H. oiapoquense* (Nijssen, 1972), *H. parallelum* (Burgess, 1993), *H. pavanelliae* (Tencatt & Ohara, 2016), *H. polystictum* (Regan, 1912), *H. schwartzi*, *H. surinamense* (Nijssen, 1970), *H. tenebrosum*, *H. trilineatum* (Cope, 1872), and *H. xinguense* (Nijssen, 1972) by having the belly with small to relatively large coalescent platelets, forming a typical mosaic-like pattern (*vs.* platelets on the belly, when present, small-sized and not coalescent, not forming a mosaic-like pattern); from *H. araguaiaense*, *H. eversi*, *H. granti*, *H. julii*, *H. pavanelliae*, *H. polystictum*, *H. trilineatum*, and *H. xinguense* for possessing a large, smoothly arched dark brown or black patch extending from the anterior portion of parieto-supraoccipital towards the region of interopercle, transversally crossing the

orbit and forming a typical mask-like blotch (*vs.* mask-like blotch absent); from *H. evelynae*, *H. parallelum*, *H. schwartzi*, *H. surinamense*, and *H. tenebrosum*, plus *H. granti*, *H. julii*, *H. pavanelliae*, and *H. trilineatum*, by the absence of dark brown or black stripes on flanks (*vs.* presence of at least one dark stripe on flanks); from *H. burgessi*, *H. colossus*, *H. melanistium*, and *H. noxium*, plus *H. evelynae*, *H. parallelum*, *H. surinamense*, and *H. tenebrosum*, by the absence of a large dark brown or black patch around dorsal-fin base (*vs.* presence of a large dark patch at least around anterior portion of the dorsal-fin base); from *H. concolor* and *H. esperanzae*, plus *H. colossus*, *H. parallelum*, and *H. pavanelliae*, by possessing infraorbital 2 in direct contact with pterotic-extrascapular, or almost in direct contact, with its posterodorsal edge clearly surpassing the suture between sphenotic and pterotic-extrascapular in a vertical (*vs.* infraorbital 2 not contacting the pterotic-extrascapular, nor its posterodorsal edge surpasses the suture between sphenotic and pterotic-extrascapular in a vertical); from *H. oiapoquense*, plus *H. araguaiaense*, *H. evelynae*, *H. julii*, *H. schwartzi*, *H. surinamense*, and *H. trilineatum*, by the absence of conspicuous dark markings on caudal fin (*vs.* caudal fin with conspicuous dark brown or black markings); from *H. kanei*, plus *H. araguaiaense*, *H. evelynae*, *H. eversi*, *H. julii*, *H. noxium*, *H. melanistium*, *H. pavanelliae*, *H. schwartzi*, *H. surinamense*, *H. tenebrosum*, *H. trilineatum*, and *H. xinguense*, by having the lateral body plates, especially of the dorsolateral series, with conspicuous concentration of dark brown or black chromatophores, with small dark blotches on flanks slightly darker than the ground color of plates (*vs.* dorso- and ventrolateral body plates with pale yellow or beige background coloration, with small dark blotches on flanks conspicuously standing out from the ground color of plates; small dark blotches on flanks variably absent in *H. tenebrosum*).

Description. Morphometric data in Tab. 2. Head laterally compressed with convex dorsal profile, roughly triangular in dorsal view. Snout intermediate long and somewhat straight; short and rounded in some specimens. Head profile convex from tip of snout to anterior nares, ascending nearly straight or slightly convex from this point to dorsal-fin origin; region of anterior portion of mesethmoid and/or region of frontal fontanel variably slightly concave. Profile nearly straight to slightly convex along dorsal-fin base. Postdorsal-fin body profile slightly concave to adipose-fin spine, concave from this point to caudal-fin base; region between dorsal and preadipose platelets typically nearly straight. Ventral profile of body nearly straight or slightly convex from isthmus to pectoral girdle, and slightly convex from this point until pelvic girdle. Profile nearly straight to slightly convex from pelvic girdle to base of first anal-fin ray, ascending concave until caudal-fin base. Body roughly elliptical in cross section at pectoral girdle, gradually becoming more compressed toward caudal fin. Highest body depth at vertical through anterior dorsal-fin origin.

Eye rounded, located dorsolaterally on head. Orbit delimited anteriorly by lateral ethmoid, anterodorsally by frontal, posterodorsally by sphenotic, posteroventrally by infraorbital 2, and anteroventrally by infraorbital 1 (Fig. 13A). Anterior and posterior nares close to each other, separated only by flap of skin. Anterior naris tubular. Posterior naris close to anterodorsal margin of orbit, separated from it by distance similar to naris diameter. Mouth small, subterminal, width similar to bony orbit diameter; skin fold extending from region just dorsolateral to mouth towards anteroventral portion of preopercle, forming lateral fold at anteroventral portion of snout; lateral fold entirely

TABLE 2 | Morphometric data of the holotype and 19 paratypes of *Hoplisoma jujuba*. SD = Standard deviation.

	Holotype	Low–High	Mean±SD
Standard length (mm)	44.4	29.2–44.4	
Percent of standard length			
Depth of body	41.4	40.1–44.8	42.1±1.3
Predorsal distance	55.2	51.4–56.6	53.9±1.4
Prepelvic distance	50.0	47.7–50.7	49.0±0.8
Preanal distance	83.3	81.8–84.3	83.0±0.8
Preadipose distance	86.9	85.6–89.4	87.3±0.9
Length of dorsal spine	30.4	25.6–33.2	30.5±2.1
Length of pectoral spine	29.3	28.5–33.4	31.3±1.5
Length of adipose-fin spine	6.8	6.4–8.9	7.4±0.7
Depth of caudal peduncle	13.3	13.3–16.4	15.2±0.7
Length of dorsal-fin base	17.8	16.6–19.5	18.2±0.8
Dorsal to adipose distance	20.0	17.9–22.6	20.0±1.1
Maximum cleithral width	29.1	28.0–31.5	29.2±0.9
Length of outer mental barbel	10.1	8.7–17.2	13.9±2.1
Head length	48.6	45.0–49.8	47.4±1.4
Percent of head length			
Head depth	82.4	80.6–89.1	84.5±2.0
Least interorbital distance	30.1	29.0–33.8	31.3±1.3
Horizontal orbit diameter	20.4	20.4–24.6	22.6±1.1
Snout length	38.9	34.3–40.4	37.9±1.5
Least internarial distance	16.2	15.0–18.7	16.7±0.8

fleshy, short, not reaching anterior margin of orbit in a vertical, its posterior portion expanded laterally, forming ventrolateral groove; area at mouth corner, just ventral to anterior portion of lateral fold, with small, wrinkle of skin; posteroventral margin of maxillary bulb with conspicuous roughly rounded to triangular fleshy expansion; dorsal portion of maxillary bulb typically smooth, or with small, roughly triangular skin flap; posterolateral margin of lower lip poorly to moderately developed, roughly straight or slightly rounded to triangular. Outer mental barbel ranging from moderately developed, not reaching anteroventral limit of gill opening, to well developed, slightly surpassing anteroventral limit of gill opening. Maxillary barbel typically slightly longer than outer mental barbel, or similar in size; slightly shorter than outer mental barbel in some specimens, apparently due to ongoing regeneration; small, roughly rounded to triangular mesial skin fold from posteroventral portion of upper lip to anteroventral portion of barbel. Inner mental barbel fleshy, base of each counterpart slightly separated from each other; mesial notch shallow, or deep. Small rounded papillae covering entire surface of all barbels, upper and lower lips, snout and isthmus.

Mesethmoid moderate in size, its length slightly smaller than frontal length; anterior tip roughly straight in lateral view, relatively short, slightly smaller than 50% of bone length; posterior margin narrow, its width clearly smaller than maximum width of

posterior portion of bone; base short, lateral posterodorsal expansion with relatively wide roughly trapezoid external projection, emerging slightly distant to distal point of suture with frontal; external projection long, its distal tip reaching to or slightly surpassing lateral edge of nasal bone; posterodorsal portion partially exposed and bearing small odontodes, or entirely covered by thick layer of skin; posterior ventrolateral expansion partially visible in dorsal view, emerging slightly anteriorly to external projection of lateral posterodorsal expansion (Figs. 13B, 14A). Upper and lower jaws edentulous; premaxilla overall funnel-like shaped, with anteroventral surface roughly triangular in frontal view; anteroventral margin irregular; posterodorsal portion with conspicuous pointed process, mesially set in frontal view (Fig. 15A); maxilla elongated, relatively slender and roughly hatchet shaped in frontal view, its proximal half with roughly triangular to trapezoid laminar process on posterolateral portion (Fig. 15A); dentary relatively slender, with roughly trapezoid expansion on its anteroventral portion, in ventrolateral perspective, smoothly bent anteriorly, directed mesially, with distal edge variably smoothly curved posteriorly; roughly triangular process on its posterodorsal portion, bent posteriorly; angulo-articular slender, with rounded dorsal laminar expansion, or moderately deep in middle portion, with rounded dorsal laminar expansion, deepest area slightly posterior to posterodorsal margin of dentary; posteroventral portion with roughly triangular process, in lateral view, bent posteriorly (Fig. 15B). Palatine longitudinally elongated, moderate-sized, with roughly triangular or trapezoid dorsolateral laminar expansion on its posterior portion, articulating with lateroventral expansion of posterior portion of mesethmoid; posterolateral process well developed, extending posteriorly in parallel to dorsal margin of anterior laminar expansion of metapterygoid (Fig. 15C).

Nasal capsule delimited posteriorly and dorsally by frontal, anteriorly by mesethmoid, and ventrally and posteriorly by lateral ethmoid. Nasal slender, laterally curved, inner margin with moderately-developed laminar expansion, typically contacting frontal and mesethmoid; outer margin with strongly reduced laminar expansion (Figs. 13B, 14). Lateral ethmoid moderately deep in lateral view, typically partially exposed anteriorly, bearing small odontodes, or entirely covered by thick layer of skin; posterior portion with relatively wide roughly triangular posteroventral expansion, and relatively long and wide roughly trapezoid posterodorsal expansion; discrete anterodorsal expansion, its posterodorsal portion relatively close from nasal, and anterodorsal margin contacting external projection of lateral posterodorsal expansion of mesethmoid; anteroventral expansion moderately developed, moderately expanded anteroventrally, contacting ventrolateral expansion of posterior portion of mesethmoid by means of large cartilage block (Fig. 13B). Frontal elongated, narrow, width less than half of entire length; anterior projection typically exposed and bearing small odontodes (Fig. 14B). Frontal fontanel relatively large, slender, and somewhat ellipsoid; posterior tip extension slightly surpassing anterior margin of parieto-supraoccipital (Figs. 13A, 14B). Sphenotic somewhat trapezoid, contacting parieto-supraoccipital dorsally, pterotic-extrascapular posteriorly, second infraorbital posteroventrally and frontal anteriorly (Fig. 13A). Pterotic-extrascapular roughly pipe-shaped, with posteriormost portion contacting first lateral-line ossicle, posteroventral margin contacting cleithrum, and anteroventral margin contacting opercle and typically infraorbital 2; anteroventral margin close but not in direct contact with infraorbital 2 in some specimens; posterior expansion almost entirely covering lateral opening of swimbladder capsule, leaving slender area on its

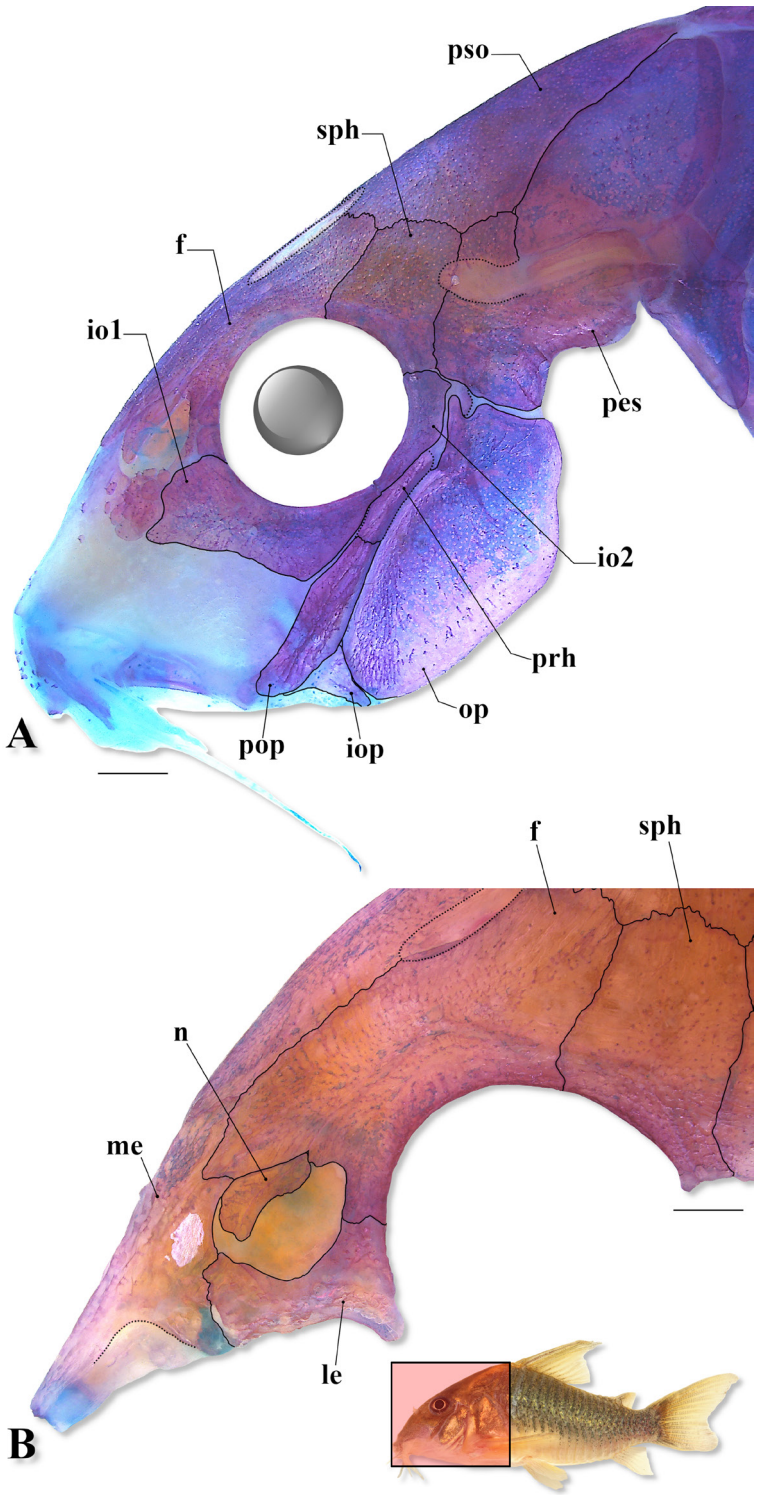

FIGURE 13 | Head osteological pattern in c&s paratypes of *Hoplisoma jujuba*, showing (**A**) the general morphology in lateral view in CITL 1736, 40.0 mm SL, and (**B**) the anterior portion of neurocranium in lateral view in CITL 1737, 42.9 mm SL. Abbreviations: f: frontal, io1–2: infraorbital 1 and 2, iop: interopercle, le: lateral ethmoid, n: nasal, me: mesethmoid, op: opercle, pes: pterotic-extrascapular, pop: preopercle, prh: posterodorsal ridge of hyomandibula, pso: parieto-supraoccipital, sph: sphenotic. Area where the illustrated bones are located in fish's body marked in red in the miniature photo in life of the holotype of the new species in lateral view. Scale bars = 1 mm.

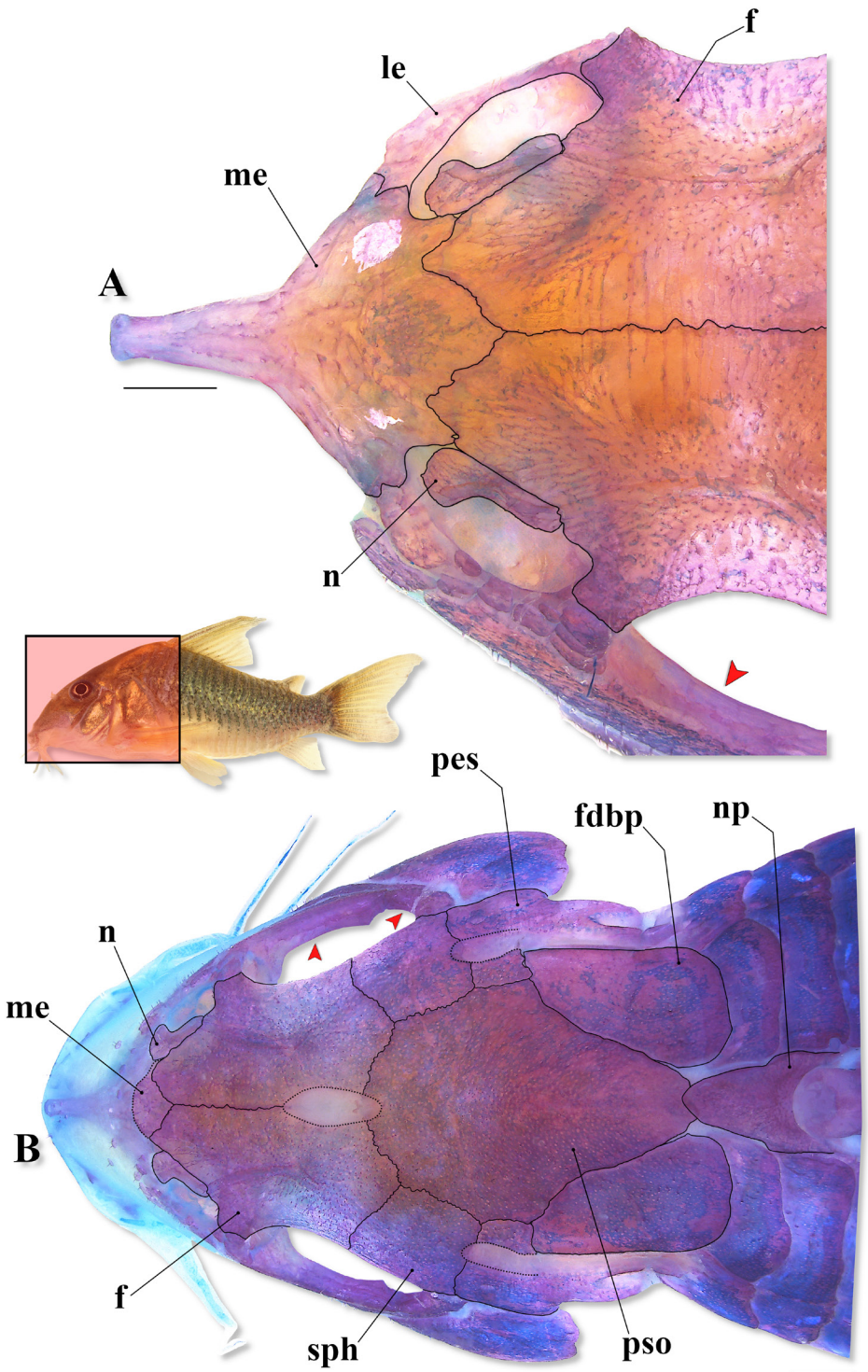

FIGURE 14 | Cranial osteology in c&s paratypes of *Hoplisoma jujuba*, showing (A) the anterior portion of neurocranium in CITL 1737, 42.9 mm SL, and (B) the predorsal portion of body in CITL 1736, 40.0 mm SL, both in dorsal view. Abbreviations: f: frontal, fdbp: first dorsolateral body plate, le: lateral ethmoid, me: mesethmoid, n: nasal, np: nuchal plate, pes: pterotic-extrascapular, pso: parieto-supraoccipital, sph: sphenotic. Red arrows indicate inner laminar expansion of both infraorbitals. Area where the illustrated bones are located in fish's body marked in red in the miniature photo in life of the holotype of the new species in lateral view. Scale bars = 1 mm.

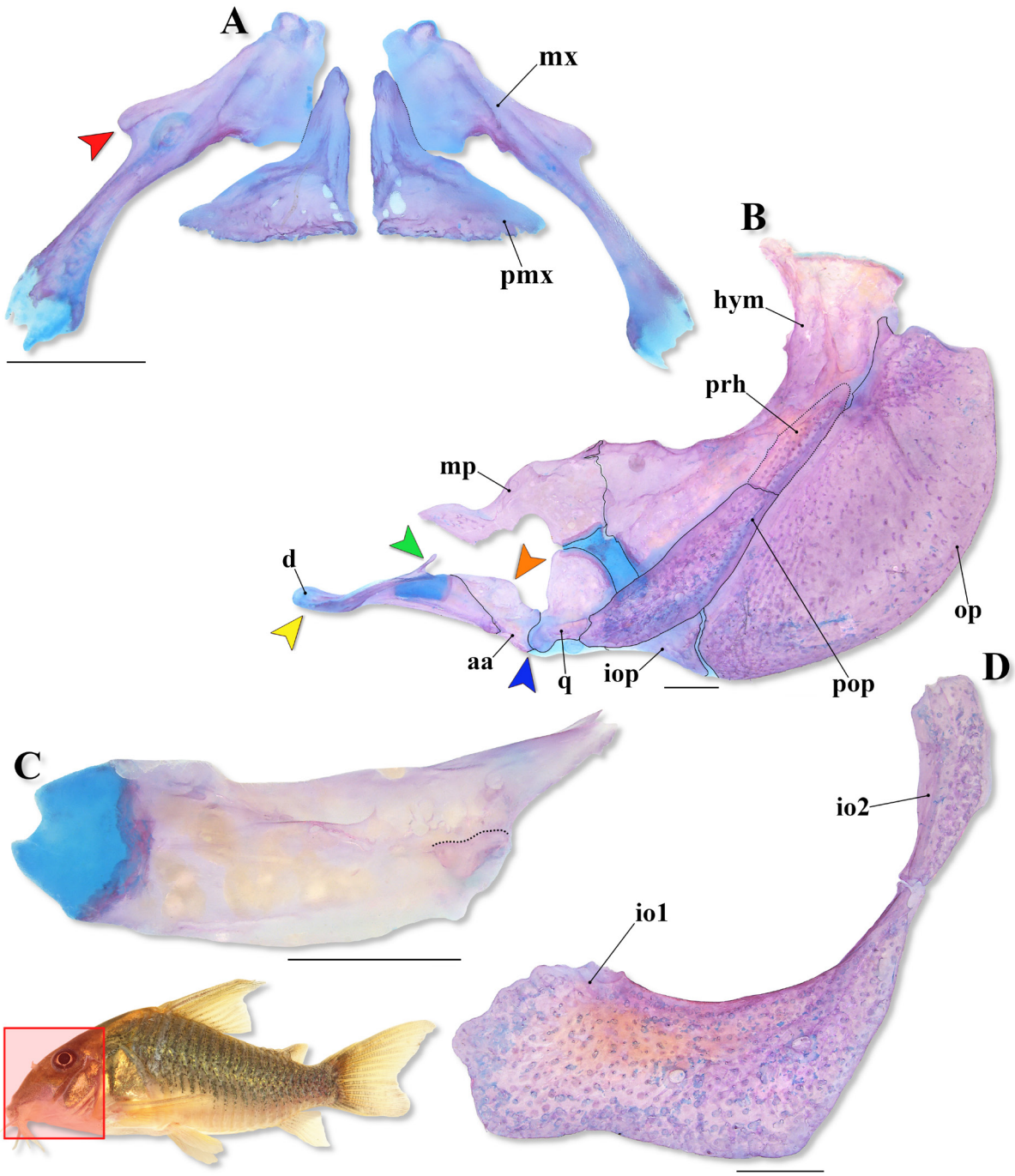

FIGURE 15 | Cranial osteology in a c&s paratype of *Hoplisoma jujuba* (CITL 1737, 42.9 mm SL), showing (**A**) the upper jaw in frontal view (= dorsal view considering everted mouth), (**B**) the suspensorium plus operculum in lateral view, (**C**) the palatine in dorsal view, and (**D**) the infraorbital series in lateral view. Abbreviations: aa: angulo-articular, d: dentary, hym: hyomandibula, io1–2: infraorbital 1 and 2, iop: interopercle, mp: metapterygoid, mx: maxilla, op: opercle, pmx: premaxilla, pop: preopercle, prh: posterodorsal ridge of hyomandibula, q: quadrate. Red arrow indicates laminar process on posterolateral portion of maxilla; yellow and green arrows indicate anteroventral expansion (not visible in this perspective) and posterodorsal process of dentary, respectively; orange and blue arrows indicate dorsal laminar expansion and posteroventral process of angulo-articular, respectively. Dotted line in (**C**) outlining dorsolateral longitudinal laminar expansion of palatine. Area where the illustrated bones are located in fish's body marked in red in the miniature photo in life of the holotype of the new species in lateral view. Scale bars = 1 mm.

dorsal margin covered only by thick layer of skin (Fig. 13A). Parieto-supraoccipital wide, posterior process long, contacting nuchal plate; region of contact between posterior process and nuchal plate covered by thick layer of skin (Figs. 13A, 14B).

Two laminar infraorbitals with minute odontodes. Infraorbital 1 large, ventral laminar expansion typically well-developed, or moderately developed (Figs. 13A, 15D); some smaller specimens (up to about 30.0 mm SL) with ventral laminar expansion poorly developed; anterior portion typically with conspicuously well-developed laminar expansion, reaching to or slightly surpassing anterior margin of nasal capsule; inner laminar expansion poorly developed (Fig. 14). Infraorbital 2 small, relatively slender, with posterior laminar expansion typically moderately developed, or poorly developed (Figs. 13A, 15D); posteroventral margin contacting posterodorsal ridge of hyomandibula, posterior margin close but not in direct contact with opercle, and posterodorsal edge contacting sphenotic and pterotic-extrascapular; posterodorsal edge clearly surpassing suture between sphenotic and pterotic-extrascapular at vertical, almost directly contacting pterotic-extrascapular in some specimens (Fig. 13A); posterodorsal portion smooth or with roughly triangular expansion, and middle portion with poorly-developed and rounded to roughly triangular expansion; inner laminar expansion poorly developed (Figs. 13A, 14B, 15D). Posterodorsal ridge of hyomandibula close to its articulation with opercle slender, exposed, and bearing small odontodes (Figs. 13A, 15B). Dorsal ridge of hyomandibula between pterotic-extrascapular and opercle covered by thick layer of skin, variably exposed and bearing small odontodes. Interopercle typically entirely covered by thick layer of skin; subtriangular, anterior projection well developed (Figs. 13A, 15B). Preopercle elongated, relatively slender; minute odontodes on external surface (Figs. 13A, 15B). Opercle dorsoventrally elongated, with width slightly smaller than half of its entire length; free margin convex, without serrations and covered by small odontodes (Figs. 13A, 15B).

Four branchiostegal rays decreasing in size posteriorly. Hypobranchial 1 deep; hypobranchial 2 somewhat triangular, tip ossified and directed towards anterior portion, posterior margin cartilaginous; ossified portion well developed, its size about twice cartilaginous portion. Five ceratobranchials with expansions increasing posteriorly; ceratobranchial 1 with small process on anterior margin of mesial portion; ceratobranchial 3 notched on postero-lateral margin; variably with continuous laminar expansion on postero-lateral margin; ceratobranchial 5 toothed on posterodorsal surface, with 45 to 51(2) teeth aligned in one row. Four epibranchials with similar size; epibranchial 2 slightly larger than others, with small, pointed process on laminar expansion of posterior margin, variably with notch just ventral to process; epibranchial 3 with roughly triangular uncinate process on laminar expansion of posterior margin, bent mesially. Two wide pharyngobranchials (3 and 4); pharyngobranchial 3 with reduced roughly straight to rounded laminar expansion on posterior margin; laminar expansion variably notched. Upper tooth plate roughly oval, 56 to 57(2) teeth aligned in two rows on posteroventral surface; rows closely aligned.

Lateral-line canal reaching cephalic laterosensory system through pterotic-extrascapular, branching twice before reaching sphenotic: pterotic branch, with single pore, preoperculomandibular branch conspicuously reduced, with single pore opening at postotic main canal; postotic main canal widens just posterior to pterotic branch. Sensory canal continuing through pterotic-extrascapular, reaching sphenotic as temporal canal,

which splits into two branches: one branch giving rise to infraorbital canal, other branch connecting to frontal through supraorbital canal, both with single pore. Supraorbital canal branched, running through nasal bone. Epiphyseal branch conspicuously reduced; pore opening close to supraorbital main canal, directed towards frontal fontanel. Nasal canal with three openings, first on posterior edge, second on posterolateral portion, variably fused with first pore, and third on anterior edge. Infraorbital canal running through entire infraorbital 2, extending to infraorbital 1 and typically opening into two pores, or in three pores. Preoperculomandibular branch giving rise to preoperculomandibular canal, which runs through almost entire preopercle with three openings, leading to pores 3, 4, and 5, respectively.

Dorsal fin subtriangular, typically located just posterior to second dorsolateral body plate. Dorsal-fin rays II,8*(20), with first branched ray as longest fin element; branched rays decreasing in size posteriorly, with first and variably second branched rays slightly longer than ossified portion of dorsal-fin spine, remaining rays with similar size or shorter than spine; branched rays on middle portion of dorsal fin smaller than adjacent rays in some specimens, forming notch on dorsal-fin posterior margin; first branched ray clearly more elongated than spine in some specimens; posterior margin of dorsal-fin spine with 15 to 21 strongly reduced to poorly-developed serrations; most serrations antrorse; some serrations variably perpendicularly directed (relative to main axis of spine), especially on distal portion of spine; serrations absent close to origin of spine, and variably on distal portion of spine; small odontodes on anterior and lateral surfaces of spine (Fig. 16A). Nuchal plate moderately developed, almost entirely exposed, with minute odontodes. Spinelet short; spine typically well developed, with adpressed distal tip clearly surpassing dorsal-fin terminus. Pectoral fin roughly triangular, its origin just posterior to gill opening. Pectoral-fin I,7,i*(12), I,8(5), I,8,i(2), I,9(1), with first branched ray as longest fin element; branched rays decreasing in size posteriorly, with first branched ray slightly longer than ossified portion of pectoral-fin spine, remaining rays with similar size or shorter than spine; posterior margin of pectoral spine with 34 to 42 strongly reduced to poorly-developed serrations along almost its entire length, absent close to origin of spine; most serrations antrorse, with some serrations perpendicularly directed (relative to main axis of spine) and/or bifid; serrations fused at base variably present, especially on distal portion of spine; perpendicularly directed serrations typically on distal portion of spine; small odontodes on anterior, dorsal and ventral surfaces of spine (Fig. 16B). Anteroventral portion of cleithrum and anterolateral portion of scapulocoracoid exposed; posterolateral portion of scapulocoracoid moderately developed, exposed, with anterior portion typically slightly expanded anteriorly, its anterior edge relatively distant from anteroventral portion of cleithrum; exposed areas bearing small odontodes. Opening of axillary gland located just posterior to pectoral-fin spine base.

Pelvic fin oblong, located just below first or second ventrolateral body plate, and at vertical through dorsal-fin spine or first dorsal-fin branched ray. Pelvic-fin rays i,5*(20); second branched ray typically as longest fin element, with rays decreasing in size towards both anterior and posterior margins of fin; first and third branched ray variably as long as second branched ray; unbranched ray typically as shorter fin element, fifth branched ray variably similar in size to unbranched ray. Anterior internal process of basipterygium well developed and ranging from moderately to conspicuously laterally expanded, with obliquely placed dorsal lamina, converging mesially towards

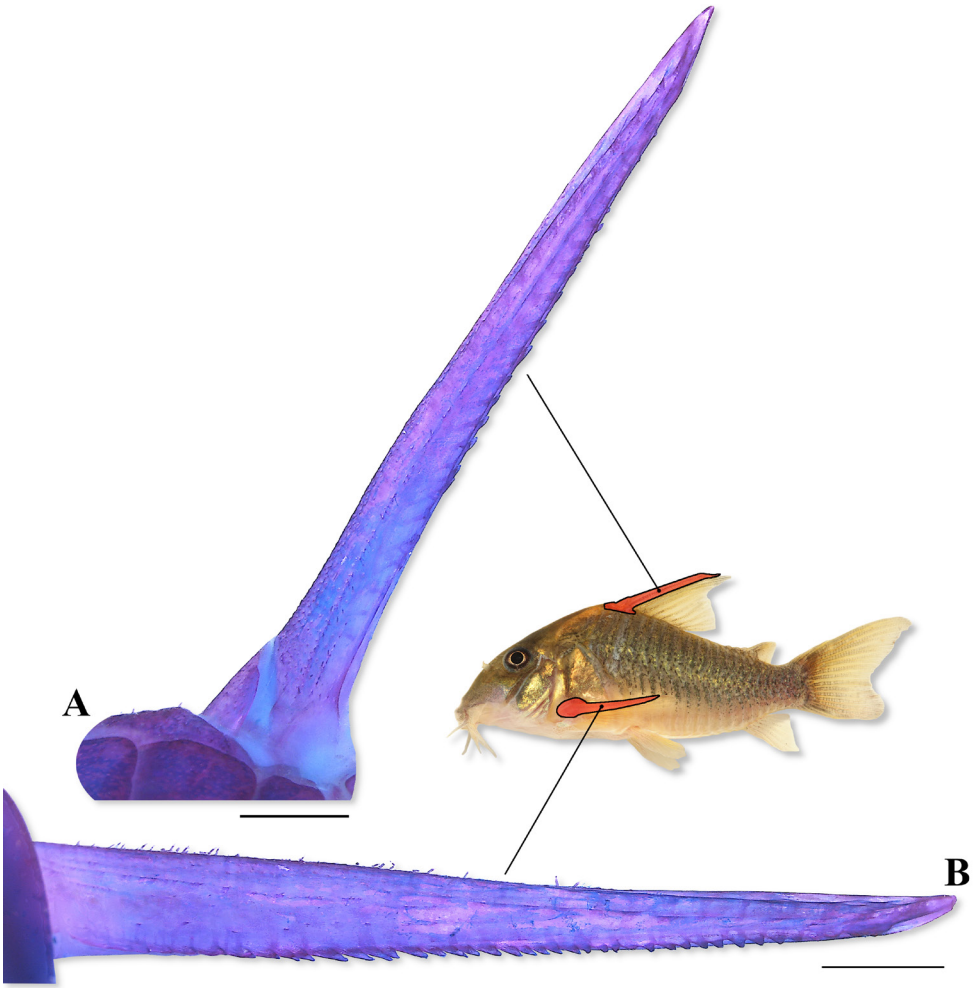

FIGURE 16 | Lateral view of (**A**) the dorsal-fin spine and dorsal view of (**B**) the right pectoral-fin spine in a c&s paratype of *Hoplisoma jujuba* (CITL 1736, 40.0 mm SL), showing their serration patterns. Area where the illustrated bones are located in fish's body marked in red in the miniature photo in life of the holotype of the new species in lateral view. Scale bars = 1 mm.

anterior edge of process, with counterparts contacting each other anteriorly, roughly triangular in lateral view, curved posteriorly, slightly bent laterally; ventral laminar expansion obliquely placed, smoothly converging mesially towards anterior edge of process, clearly less developed than dorsal lamina; anterior external process falciform, well developed and conspicuously expanded posteriorly, with conspicuous notch on its anterolateral portion; dorsal ischiac process conspicuously well developed, with anterior laminar expansion irregular, conspicuously expanded anteriorly, and posterior laminar expansion roughly triangular, conspicuously expanded posteriorly; posterior edge of anterior external process contacting anterior edge of dorsal ischiac process in some specimens; ventral ischiac process clearly smaller than dorsal process, roughly triangular, bent anteriorly (Fig. 17). Adipose fin roughly triangular, separated from base of last dorsal-fin ray by six or seven dorsolateral body plates. Anal fin subtriangular, located just posterior to 12th or 13th ventrolateral body plates, and typically at vertical

through adipose-fin spine base. Anal-fin rays ii,5,i(9), ii,6(8), i,7*(2), single specimen with ii,3,i,2, possibly due to malformation; third ray typically as longest fin element, with rays decreasing in size towards both anterior and posterior margins of fin; first or last ray as shorter fin element. Caudal fin bilobed, with dorsal and ventral lobes similar in size or dorsal lobe slightly larger than ventral lobe; some specimens undergoing caudal regeneration with dorsal lobe smaller than ventral lobe. Caudal-fin rays i,11,i(1), i,12,i*(19), with generally four or five dorsal and ventral procurrent rays increasing in size posteriorly; small cartilage between upper principal and procurrent caudal-fin rays not observed (Fig. 18).

Typically, three laterosensory canals on trunk; first ossicle tubular, second ossicle laminar, both bearing small odontodes; third encased in third dorsolateral body plate. Body plates with minute odontodes scattered over exposed area, with conspicuous line of odontodes confined to posterior margins. Dorsolateral body plates 22(1), 23*(19); ventrolateral body plates 20*(15), 21(5). Dorsolateral body plates along dorsal-fin base 5(4), 6*(16); dorsolateral body plates between adipose- and caudal-fin 6(2), 7*(17), 8(1). Preadipose platelets 2(2), 3*(15), 4(3). Ventral surface of trunk between posteroventral margin of cleithrum and pelvic-fin origin typically laterally delimited only by first ventrolateral body plate; ventral portion of first ventrolateral body plate ranging from slightly to moderately expanded anteriorly. Small platelets covering base of caudal-fin

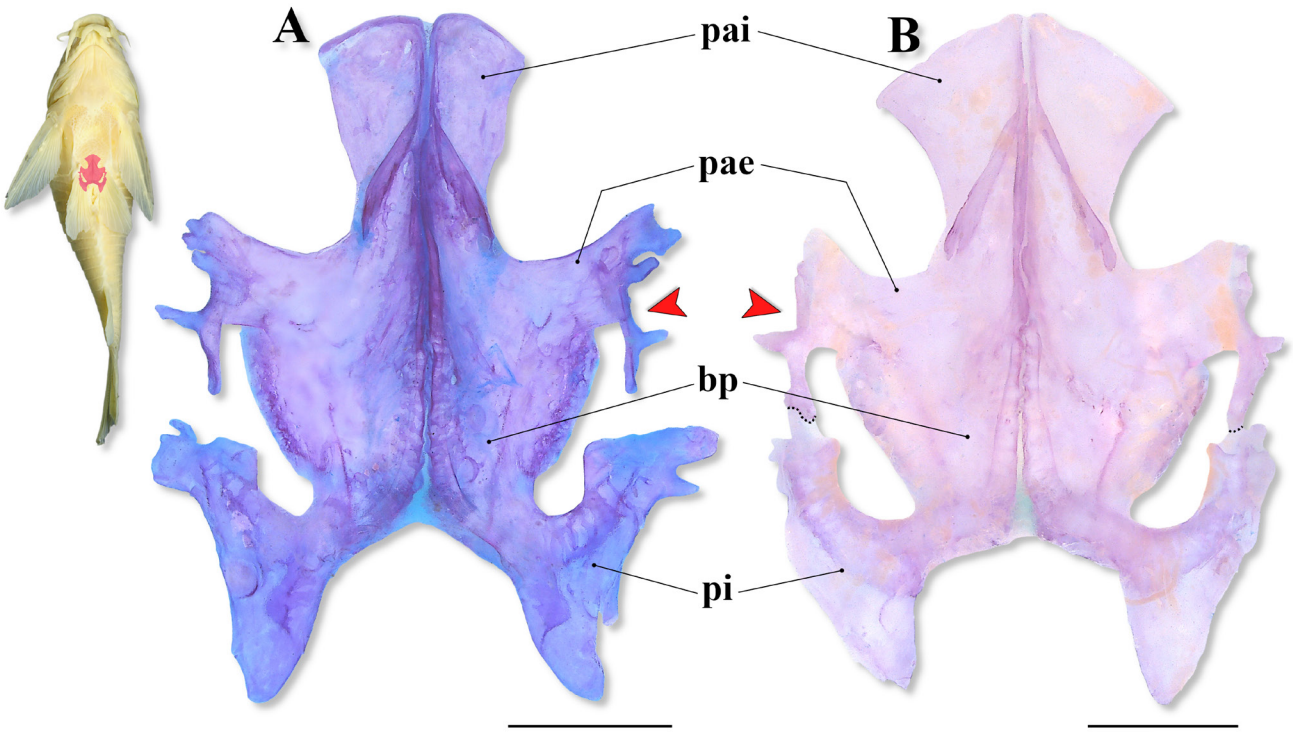

FIGURE 17 | Pelvic girdle in c&s paratypes of *Hoplisoma jujuba*, showing (**A**) the specimen CITL 1736, 40.0 mm SL, lacking contact between the posterior edge of anterior external process and the anterior edge of dorsal ischiac process, and (**B**) the specimen CITL 1737, 42.9 mm SL, with the posterior edge of anterior external process contacting the anterior edge of dorsal ischiac process (dotted lines). Abbreviations: bp: basipterygium, pae: anterior external process, pai: anterior internal process, pi: dorsal ischiac process. Red arrows indicating the anterolateral notch of the anterior external process. Area where the illustrated bones are located in fish's body marked in red in the miniature photo of the preserved holotype of the new species in ventral view. Scale bars = 1 mm.

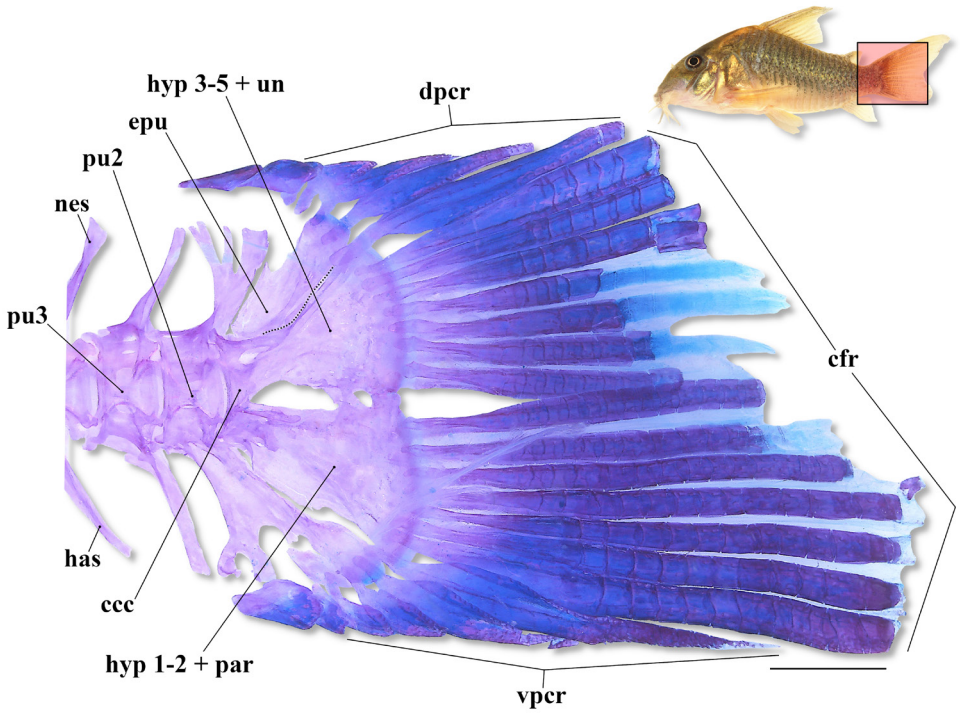

FIGURE 18 | General morphology of caudal skeleton in a c&s paratype of *Hoplisoma jujuba* (CITL 1736, 40.0 mm SL). Abbreviations: ccc: compound caudal centrum, cfr: caudal-fin principal rays, dpcr: dorsal procurrent rays, epu: epural, has: haemal spine, hyp 1–5: hypurals 1 to 5, nes: neural spine, par: parhypural, pu 2–3: preural centra 2 to 3, un: uroneural, vpcr: ventral procurrent rays. Area where the illustrated bones are located in fish's body marked in red in the miniature photo in life of the holotype of the new species. Scale bar = 1 mm.

rays; small platelets disposed dorsally and ventrally between junctions of lateral plates on posterior portion of caudal peduncle. Anterior margin of orbit, above region of junction between frontal and lateral ethmoid, region around nasal capsule, anterior and posterior portions of mesethmoid, and anteroventral surface of snout above premaxilla and proximal portion of maxilla variably with small to relatively large platelets bearing odontodes. Belly typically mostly covered by small- to relatively large-sized coalescent platelets, forming typical mosaic-like pattern; platelets irregular in shape and bearing odontodes; some smaller specimens (up to about 35.0 mm SL) with smaller patches of mosaic-like platelets, presenting moderate-sized to large naked areas on belly (Fig. 19).

Vertebral count 21(1), 22(1); ribs 7(2); first pair conspicuously large, its middle portion closely connected to first ventrolateral body plate; its tip connected to anterior external process of basipterygium. Parapophysis of complex vertebra well developed.

Coloration in alcohol. Overall color pattern of body in Fig. 12. Ground color of body pale- to brownish yellow or beige. Top of head dark brown. Dorsal and lateral surface of head covered by dark brown or black chromatophores, typically not forming small blotches; small, diffuse dark blotches on lateral surface of head in some specimens, especially on its posterior portion; lips and barbels with dark brown

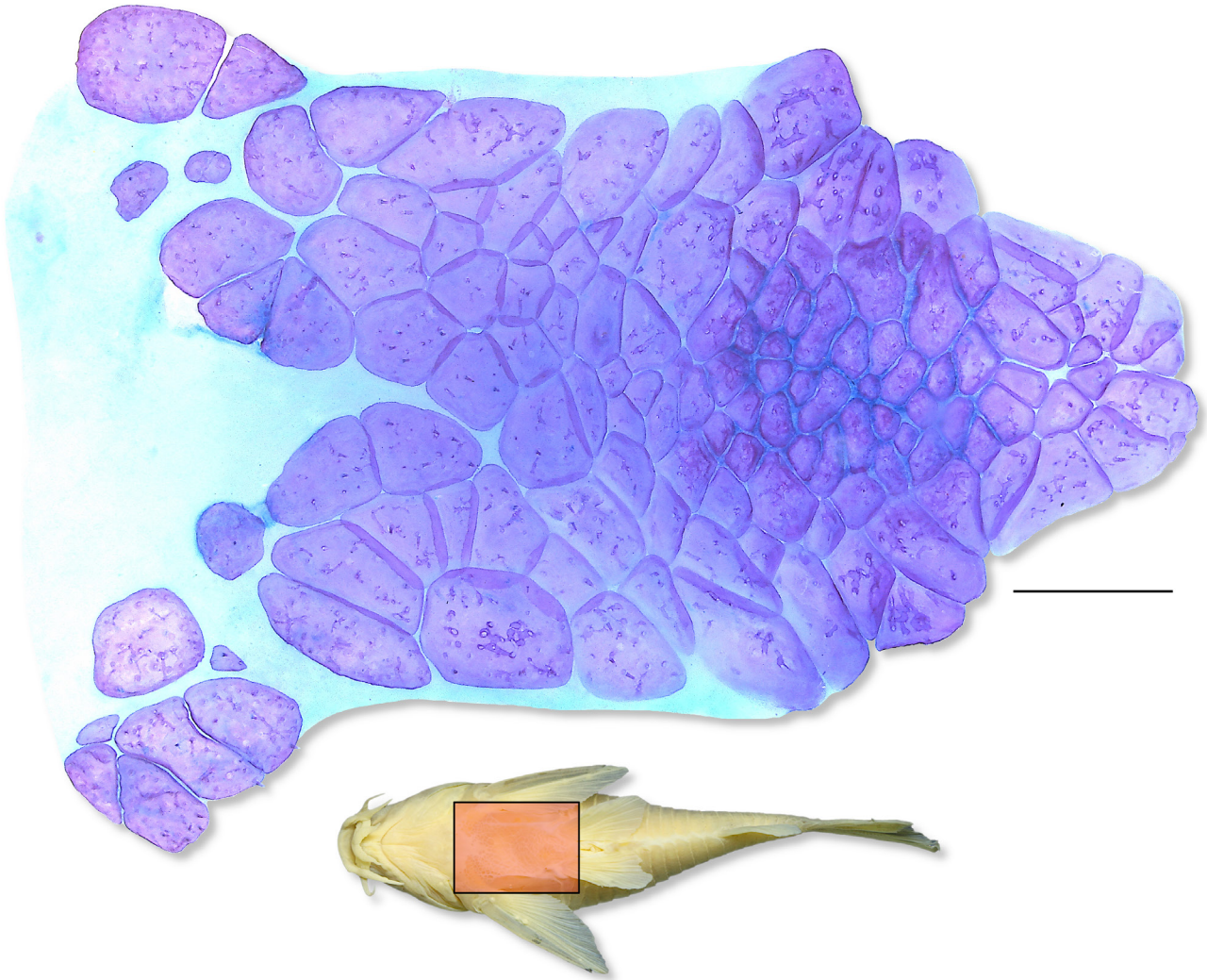

FIGURE 19 | Ventral surface of trunk in a c&s paratype of *Hoplisoma jujuba* (CITL 1736, 40.0 mm SL), showing the small to relatively large, coalescent irregular platelets, forming the typical mosaic-like pattern on the belly. Area where the illustrated structures are located in fish's body marked in red in the miniature photo of the preserved holotype of the new species in ventral view. Scale bar = 1 mm.

or black chromatophores, conspicuously more concentrated on upper lip and outer mental barbel; chromatophores on inner mental barbel numerous or scarce, apparently absent in some specimens; ventrolateral portion of head variably with dark brown or black chromatophores, isthmus apparently devoid of chromatophores or with scarce dark brown or black chromatophores on anterior portion; large, smoothly arched dark brown or black patch extending from interopercle region to anterior portion of parieto-supraoccipital, transversally crossing orbit, where it meets its counterpart and extends towards posterior process of parieto-supraoccipital, forming typical mask-like blotch with V-shaped pattern in dorsal view; mask-like blotch typically diffuse, slightly distinct from surrounding areas; some specimens with more evident mask; anterior and middle portions of opercle, especially on its ventral two thirds, with more concentrated dark brown or black chromatophores, forming large, irregular dark patch

typically fused with mask-like blotch, posterior margin of bone typically lighter than surrounding areas; region of contact between posterior process of parieto-supraoccipital and first dorsolateral, and nuchal plate lighter than surrounding areas, forming V-shaped pattern in dorsal view; lateral surface of cleithrum, especially on its middle portion, with conspicuous concentration of dark brown or black chromatophores, variably forming small, rounded to irregular diffuse dark brown or black blotches. Dorsolateral body plates with conspicuous concentration of dark brown or black chromatophores, forming small, irregular, rounded or vertically elongated dark brown or black blotches, slightly darker than ground color of plates; blotches irregularly disposed or roughly vertically aligned. Ventrolateral body plates with conspicuous concentration of dark brown or black chromatophores, forming small, irregular, rounded or vertically elongated dark brown or black blotches, slightly darker than ground color of plates; blotches irregularly disposed or roughly vertically aligned; dark pigmentation gradually reducing towards ventral portion of plates, with blotches typically restricted to dorsal half of plates; region posterior to anal-fin origin with small, diffuse dark blotches on ventral half of plates in some specimens; blotches on flanks slightly more evident in few smaller specimens (up to about 35.0 mm SL). Midline of flank in some juvenile specimens (up to about 30.0 mm SL) with longitudinal series of slightly larger, diffuse, irregular or slightly vertically elongated dark blotches. Posterior margin of body plates typically with dark brown or black chromatophores, forming thin dark lines along border of plates, more evident on dorsal and middle portions of flank. Dorsal, pectoral, pelvic, anal, adipose, and caudal fins with dark brown or black chromatophores, typically not forming dark blotches; chromatophores on dorsal fin variably more concentrated on its anterior portion and/or along its base; dorsal surface of pectoral-fin base on axillary region typically with dark brown or black chromatophores; dorsal, anal, and/or caudal fins variably with small, diffuse dark blotches.

Coloration in life. Similar to color pattern of preserved specimens, but with brighter ground color of body, which can be pale yellow to beige, orangish yellow, reddish orange, or greyish yellow (Figs. 20, 21). Mask-like blotch more evident; predorsal V-shaped patch more evident, bright orange or yellow. Body covered by bluish, or greenish yellow iridescent coloration, especially on region of opercle and cleithrum. Wild-caught and some aquarium specimens typically displaying a bluish green metallic sheen on flanks (Figs. 21A–D, G); some specimens variably lacking such coloration (Figs. 20, 21E–F).

Sexual dimorphism. Male specimens of *Hoplisoma jujuba* present a genital papilla, which is somewhat tubular to conical, a condition well-documented in Corydoradinae (see Britto, 2003; Nijssen, Isbrücker, 1980; Spadella *et al*., 2017).

Geographical distribution. *Hoplisoma jujuba* is so far known from its type locality, the rio Pacu, and from the igarapé Limãozinho, both tributaries of the rio Tapajós, rio Amazonas basin, Jacareacanga Municipality, Pará State, Brazil (Fig. 10).

Ecological notes. See the "Ecological notes" section of *Brochis bodrocki*.

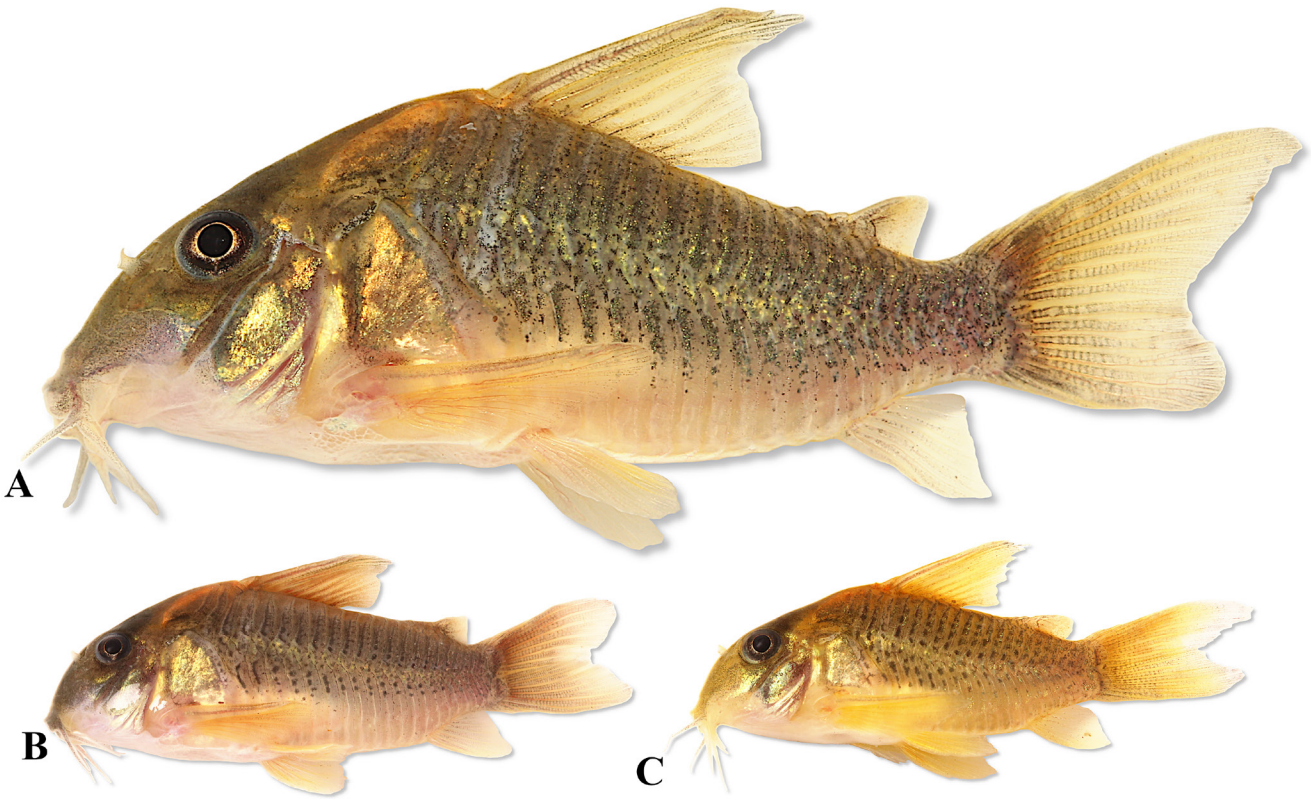

FIGURE 20 | Color pattern in life of *Hoplisoma jujuba* in lateral view, showing (**A**) the holotype (MNRJ 56197, 44.4 mm SL), and two paratypes, (**B**) INPA 62599, 43.0 mm SL, and (**C**) INPA 62599, 26.4 mm SL, showing the variations in their color pattern. Photos by WMO.

Etymology. *Hoplisoma jujuba* is named in honor of Marcos Pinheiro, also known by the nickname "jujuba" (a traditional gummy candy in Brazil), an experienced and skilled collector of Corydoradinae, also expert in other fish (Loricariidae, Cichlidae, Auchenipteridae, Acestrorhamphidae) from the region. Marcos helped to catch or obtain the specimens of both new species described herein, kindly guiding us (LFCT and WMO) during our expedition to Jacareacanga, Pará, where the type specimens of the recently *Hoplisoma noxium* and *H. tenebrosum* were also captured. A noun in apposition.

Conservation status. The new species occurs in the same sites, and consequently same region, of *B. bodrocki*. Therefore, by the same reasoning (see "Conservation status" for *B. bodrocki*) and according to the International Union for Conservation of Nature (IUCN) categories and criteria (IUCN Standards and Petitions Subcommittee, 2024), *Hoplisoma jujuba* would be classified as Least Concern (LC).

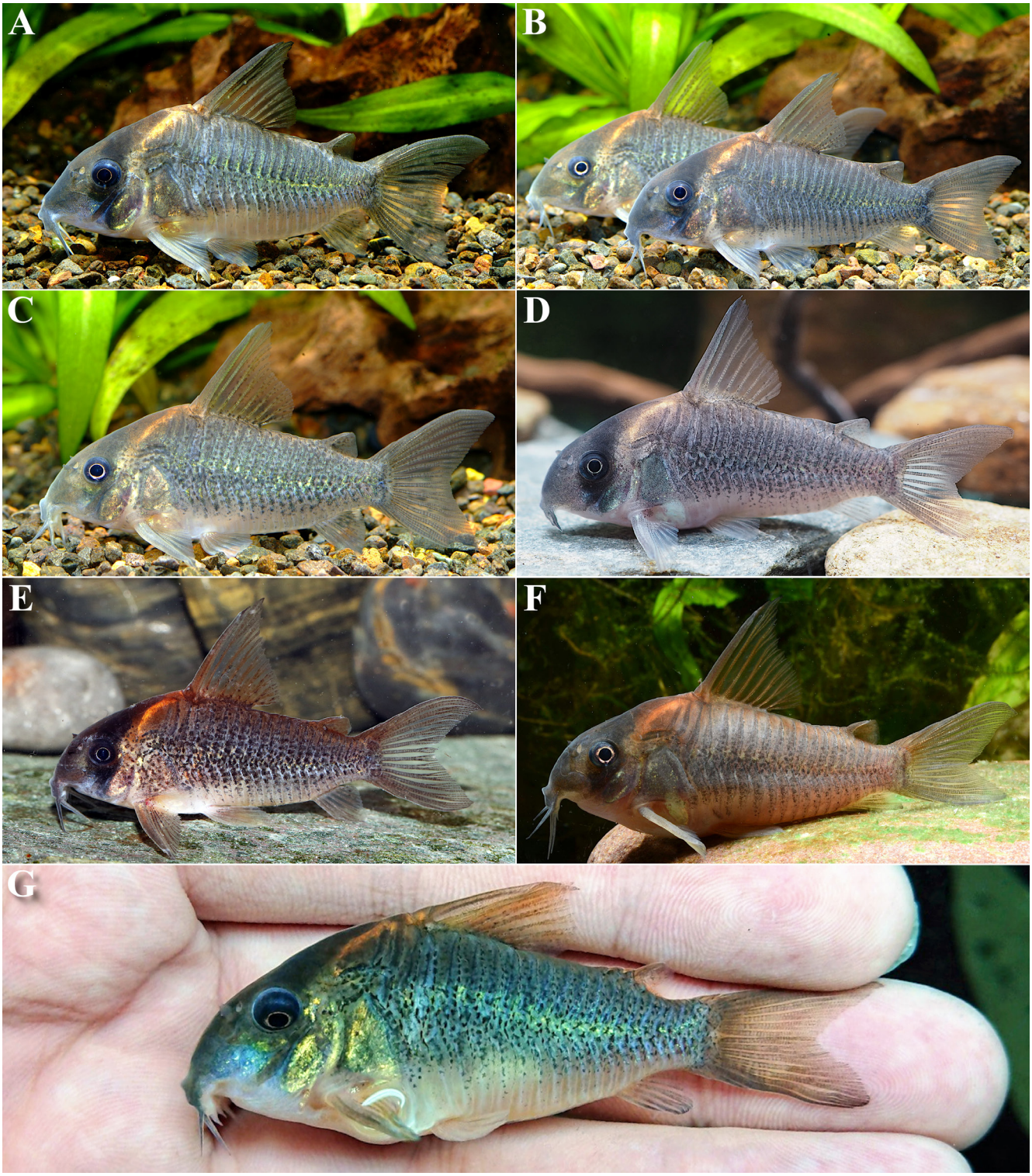

FIGURE 21 | Variation in color pattern in life in unpreserved and unmeasured aquarium specimens of *Hoplisoma jujuba* in lateral view, showing the variations in their color pattern. Photos (**A**–**C**) by Wei-Chieh Tseng, (**D**) by Haakon Haagensen, (**E**) by Ian Fuller, (**F**) by Hans Evers, and (**G**) by CP Aqua Studio.

Identification key to the valid species of Corydoradinae from the rio Tapajós basin (adapted from Tencatt *et al.*, 2022a)

1a. Two cranial fontanels..... *Aspidoras poecilus*
1b. A single cranial fontanel..... 2
2a. Posterior margin of dorsal-fin spine with most serrations retrorse 3
2b. Posterior margin of dorsal-fin spine with most serrations, when present, antrorse 5
3a. Flanks devoid of dark stripes..... *Brochis bodrocki*
3b. Flanks with two to four dark stripes..... 4
4a. Two relatively wide, dark brown or black, longitudinal stripes on flanks..... *Brochis bifasciata*
4b. Three or four slender, dark brown or black, longitudinal stripes on flanks..... *Brochis ornata*
5a. Posterior margin of pectoral-fin spine with most serrations retrorse 6
5b. Posterior margin of pectoral-fin spine with most serrations antrorse or perpendicularly directed 7
6a. Snout pointed; corner of the mouth with a roughly triangular fleshy flap ..... *Corydoras caramater*
6b. Snout markedly rounded; corner of the mouth lacking a fleshy flap ..... *Gastrodermus* cf. *pygmaeus*
7a. Body devoid of conspicuous blotches 8
7b. Body with pale and/or dark conspicuous blotches 9
8a. Posterior process of the parieto-supraoccipital not in contact with the nuchal plate ..... *Osteogaster hephaestus*
8b. Posterior process of the parieto-supraoccipital in contact with the nuchal plate ..... *Hoplisoma psamathos*
9a. Whitish to brownish yellow or pale yellow/beige blotches on body present..... 10
9b. Pale blotches absent..... 11
10a. Flanks covered by small dark blotches, which can be roughly longitudinally aligned and variably fused with each other, forming narrow irregular lines, but not solid stripes ..... *Hoplisoma noxium*
10b. Flanks with two or three conspicuous dark stripes..... *Hoplisoma tenebrosum*
11a. Dark mask-like blotch, transversally crossing the orbit, present 2
11b. Dark mask-like blotch, transversally crossing the orbit, absent..... 13
12a. Midline of flank lacking a conspicuous longitudinal series of dark blotches ..... *Hoplisoma jujuba*
12b. Midline of flank with a conspicuous longitudinal series of dark blotches ..... *Hoplisoma rikbaktsa*
13a. Anterior laminar expansion of infraorbital 1 strongly well developed, conspicuously expanded towards the anteroventral portion of snout, significantly covering its lateral surface ..... *Hoplisoma thanatos*
13b. Anterior laminar expansion of infraorbital 1 ranging from moderately to well developed, not conspicuously expanded towards the anteroventral portion of snout, leaving most of its lateral surface uncovered 14

14a. Body depth 36.9–42.6% of SL; least interorbital distance (13.8–17.3% of HL) ..... *Hoplisoma apiaka*
14b. Body depth 30.0–35.7% of SL; least interorbital distance (18.8–27.7% of HL) .. 15
15a. Body with conspicuous dark brown or black markings ..... *Hoplisoma benattii*
15b. Body lacking conspicuous dark brown or black markings; dark markings, when present, diffuse ..... *Hoplisoma hypnos*

DISCUSSION

When the two new species, and *Corydoras caramater* Tencatt, Couto, Santos & Sousa, 2024 are observed and caught in the wild, their bodies seem to reflect an iridescent blue coloration to the human eye, so much so that the fishermen call them "azulzinhas" ("little blue ones" in a free translation; LFCT, pers. obs.). After time in captivity, and in captive bred specimens, the iridescent blue fades, and in some cases is not visible at all (Hans Evers, pers. comm.; SG, pers. obs.).

There are many fishes with blue coloration (Bagnara *et al*., 2007), especially in the South American Characidae (*e.g*., Clothier, Lythgoe, 1987; Marinho *et al*., 2017; Zarske, 2008). Despite the circa 230 valid species of Corydoradinae and over 300 phenotypes/morphotypes recognized by aquarists' code numbers (Bentley *et al*., 2021) with several green- and yellow-colored species, blue body coloration in Corydoradinae is relatively rare (Fuller, Evers, 2024). The two new species and *C. caramater* are co-mimics as they are sympatric and, in some locations, syntopic. Müllerian mimicry rings (a group of individuals from at least two species that co-occur to some extent and share an honest aposematic warning signal (Chatelain *et al*., 2023)) are relatively common in Corydoradinae (Alexandrou *et al*., 2011), but no previous record of a mimicry ring sharing bluish body coloration has been formally reported for the group.

Color patterns in Corydoradinae have long been used for differentiating and helping to diagnose species, but recently closer attention has been given to the putative function of the color pattern of some of the species (Bentley *et al*., 2021; Tencatt *et al*., 2023b; Tencatt *et al*., 2025a). Given the rarity of an overall blue body coloration in a species rich subfamily, the presence of a blue-colored mimicry ring and the blue coloration fading to some extent in captivity, the coloration of the two new species and *C. caramater* warrants further discussion herein.

Color production in fish can be mainly divided into two types of chromatophores. The first group are pigmentary cells, which are usually dendritic. Pigmentary colors originate from compounds in cells that exhibit selective absorption of specific wavelengths of light, allowing light of other wavelengths to be reflected (Andrade, Carneiro, 2021) and include melanophores, xanthophores, erythrophores, and rarely, blue pigments cyanophores (Schaefer *et al*., 2015). There is also a very rare bili-binding protein pigment (sandercyanin), found in surface mucus of some fish (Schaefer *et al*., 2015). Some pigment cells rely on the pigment to be metabolized, including melanins, carotenoids, and pterins (Andrade, Carneiro, 2021). The second group is structural colors, in which the blue color is seen because the wavelengths of light that interact with their respective surfaces are dominated by blues and violets. The expression of these blue wavelengths is a function of the morphology of structures in the surface

layers and thus, the emanated colors are called structural colors (Umbers, 2013). Cells such as iridophores and leucophores both contain purines (normally guanine and uric acid respectively) (Bagnara *et al*., 2007; Kimura *et al*., 2014; Schaefer *et al*., 2015; Ligon, McCartney, 2016), some of which can emit fluorescent light (Ghosh *et al*., 2016; Hamied *et al*., 2020).

With the rare exception of cyanophores, which contain blue pigment, most blue colors in fishes are a result of light interaction from structural cells, or interplay between pigment cells and structural cells by the interplay between the melanophores, any xanthophores, or erythrophores, with that of the leucophores and/or iridophores being on different layers, *e.g*., the selective absorption of light rays of greater wavelength by the deep-seated background of melanophores, and partly to the action of the iridophores, which reflect, scatter, or diffract the waves of shorter length (Amiri, Shaheen, 2012; Umbers, 2013; Zhao *et al*., 2022). In the case of fishes containing the rare blue pigment sandercyanin, the fish appear blue when underlying yellow pigments are absent (Schaefer *et al*., 2015). In some species, *e.g*., *Paracheirodon innesi* (Myers, 1936), the iridophores can also be controlled physiologically to thicken or narrow. In one state the reflected light is blue and in the other, it is green (Clothier, Lythgoe, 1987). This phenomenon may explain why, in both new species, some of the specimens newly captured in the wild exhibited an iridescent green coloration, while others displayed a bluish sheen.

Umbers (2013) stated that for the best production of blue light (*i.e*., a more accurate display of this specific wavelength), the suspension of particles should overlay something dark, *e.g*., underlying melanin in melanophores. In the three species, when the blue fades in captivity the general body color is dark, with slightly contrasting dark spots. Whilst there has been no histology study on the three species, the weight of evidence in the literature would suggest that the blue coloration is because of interplay between underling pigment cells (likely the melanophores due to the dark pigment on the body) and overlying iridophores.

As stated above after a short while in captivity, the blue coloration fades or disappears. Color changes in teleost fishes is not unusual (Leclercq *et al*. 2010; Sköld *et al*., 2013; Ligon, McCartney, 2016; Grant, 2019). Chromatophores can be under hormonal or nervous control (Parker, 1948; Fujii, 1969). By altering the dendritic state of the pigment cells and/or changing the state of any structural cells, colors hues can be changed or essentially switched off (Umbers, 2013; Ligon, McCartney, 2016). Tencatt *et al*. (2023) discuss the different types of color-change in teleost fishes, *e.g*., Physiological Color Change (PCC) and Morphological Color Change (MCC), and detail the unusual changes in color that can be exhibited by *Hoplisoma colossus* (Tencatt *et al*., 2023). PCCs are acute transient events caused by the motility of pigment vesicles or reflective structures within their cell (Leclercq *et al*., 2010).

MCCs is unlikely to be the cause as in the natural environment it is present in adult specimens but then lost or faded in captivity. Proximate MCC is defined as "morphological modulations of a given life-stage skin color in response to occurring variations in biotic and abiotic environmental factors". Several factors can cause Proximate MCC and can be categorized further into Primary factors (nutrition, UV light) and Secondary (surrounding light, light cycle, and conspecific interactions (mainly through the melanogenic effect of stress due to subordination or territoriality)). The varying stimuli

are UV radiation, food borne substances such as carotenoids, or hormones. The partial or full loss of blue iridescence in captivity could be environmental. Tencatt *et al*. (2024a) detail the ecological conditions the blue co-mimics and their syntopics are found in, which does not appear to be markedly different to other species so it is unlikely to be due to PCC caused by water chemistry or differing wavelengths of light. As discussed above, some pigments need to be metabolized (including blue) and differences in the wild diet and that in captivity could affect some of the chromatophores and their interaction with each other, thereby affecting the color seen by humans.

Bentley *et al*. (2021) and Tencatt *et al*. (2023b, 2025a) discussed the possible positive adaptive value and multifunctional nature of color patterns in Corydoradinae, such as aposematism, crypsis, UV protection, and infraspecific (including intrasexual and intersexual) signaling. Umbers (2012) specifically discusses functions of blue colors in animals. Because blue colors often require precise development or expensive pigments, honest infraspecific signaling as an indicator of quality hypotheses are commonly invoked in studies to explain their function (Gray *et al*., 2008). Both sexes of the three Corydoradinae species exhibit blue coloration so it is unlikely to be sexual dichromatic signaling, but the directionality of iridescent colors might allow fishes to direct their signals at intended receivers, such as prospective mates or rivals but also to avoid unnecessary conflict with nearby conspecifics (Doucet, Meadows, 2009). Several studies have been made on the use of blue color for aposematism; some of which showed that it is used to deter or deflect predators (numerous examples in Cott, 1940; Sadovy *et al*., 2005), while others found no evidence to support it (Umbers, 2012). All three species in the Corydoradinae mimicry ring (*i.e*., *C. caramater*, *B. bodrocki*, and *H. jujuba*) exhibit the yellow or orange iridescent patch between the insertion of the dorsal-fin spine and pectoral-fin spine insertions (in dorsal view) that is found in *H. colossus*, which is a putative aposematic signal (Tencatt *et al*., 2023b). These highly contrasting edges would be even more vivid to predators on the darker substrates the three species can sometime be found on.

For fishes, other than in marine environments (Marshall, 2000), blue coloration for crypsis is rarely but sometimes documented (Schaefer *et al*., 2015). Birds and fishes are the natural predators of Corydoradinae (Alexandrou *et al*., 2011) and they can see the blue (and into the ultraviolet) spectrum (Jacobs, 1992) so the blue coloration may make them conspicuous to conspecifics. It may also make them conspicuous to predators (aposematism) or cryptic depending on the substrate and viewpoint of the predator. The three species live in very clear water, with some light sand substrate areas and some darker substrates. During the field observations, LFCT considered them more difficult to find or see them on the darker substrates, but also on sand their color pattern is disruptive. Based on the information about their habitat, with potential high levels of UV due to clearwater, the likely cryptic effect of their color pattern observed by LFCT on differing substrates, the putatively aposematic body color and iridescent V collar, the body of literature on blue colors (including in combination with pungent spines and toxins), it is hypothesized that the unusual blue coloration of the three co-mimics could serve a multifunctional purpose (*e.g*., UV protection, crypsis, aposematism, and potentially infraspecific and intraspecific signaling). Why these three species appear to have converged to form this blue-colored Müllerian mimicry ring and other syntopic Corydoradinae species did not, needs further investigation.

Comparative material examined. *Brochis*: *Brochis ambiacus*: ANSP 8291, holotype of *Corydoras ambiacus* Cope, 1872, 40.4 mm SL; MZUSP 26053, 2, 41.8–47.2 mm SL. *Brochis approuaguensis*: MZUSP 27895-6, 2, 43.0–46.1 mm SL, paratypes of *C. approuaguensis* Nijssen & Isbrücker, 1983. *Brochis arcuata*: BMNH 1939.3.3.1, holotype of *Corydoras arcuatus* Elwin, 1938, 43.3 mm SL. *Brochis bethanae*: MUSM 69403, holotype of *Corydoras bethanae* Bentley, Grant & Tencatt, 2021, 51.2 mm SL. *Brochis bifasciata*: MZUSP 38976, 16, 23.6–30.0 mm SL, paratypes of *Corydoras bifasciatus*. *Brochis britskii*: ZUFMS-PIS 862, 12, 72.0–78.0 mm SL. *Brochis brittoi*: MNRJ 43316, holotype of *Corydoras brittoi* Tencatt & Ohara, 2016, 38.1 mm SL. *Brochis condiscipulus*: MZUSP 38957, 7, 34.1–40.3 mm SL, paratypes of *Corydoras condiscipulus*. *Brochis crimmeni*: MZUSP 52490, holotype of *Corydoras crimmeni*, 36.1 mm SL. *Brochis difluviatilis*: MZUSP 75268, holotype of *Corydoras difluviatilis* Britto & Castro, 2002, 39.8 mm SL. *Brochis ephippifer*: MZUSP 31605, 2, 44.9–49.1 mm SL. *Brochis garbei*: MNRJ 18089, 14, 19.2–25.3 mm SL, 2 c&s, 25.9–27.4 mm SL. *Brochis heteromorphus*: USNM 204224, 2, 37.0–42.7 mm SL, paratypes of *Corydoras heteromorphus* Nijssen, 1970. *Brochis incolicana*: MZUSP 45717, holotype of *Corydoras incolicana*, 47.6 mm SL. *Brochis leopardus*: USNM 93305, lectotype of *Corydoras leopardus* Myers, 1933, 38.7 mm SL. *Brochis ornata*: USNM 216075, 1, 37.8 mm SL, paratype of *Corydoras ornatus*. *Brochis orphnopterus*: USNM 204361, holotype of *Corydoras orphnopterus*, 55.9 mm SL. *Brochis pantanalensis*: NUP 10188, 1 c&s, 46.4 mm SL; NUP 12593, 21, 38.7–51.2 mm SL. *Brochis pinheiroi*: MZUSP 48099, holotype of *Corydoras pinheiroi* Dinkelmeyer, 1995, 54.3 mm SL. *Brochis robineae*: MZUSP 27175, holotype of *Corydoras robineae* Burgess, 1983, 33.7 mm SL. *Brochis seussi*: MZUSP 49323, 10, 44.3–54.0 mm SL, paratypes of *Corydoras seussi* Dinkelmeyer, 1996. *Brochis splendens*: NUP 12990, 1, 43.7 mm SL; NUP 10195, 1 c&s, 54.6 mm SL. *Brochis virginiae*: USNM 326186, 3, 31.6–33.5 mm SL, paratypes of *Corydoras virginiae*. ***Hoplisoma*:** *Hoplisoma adolfoi*: MZUSP 26641, holotype of *Corydoras adolfoi* Burgess, 1982, 32.5 mm SL. *Hoplisoma amphibelum*: ANSP 8290, holotype of *Corydoras amphibelus* Cope, 1872, 26.4 mm SL. *Hoplisoma araguaiaense*: MZUSP 87155, 33 4, 24.9–46.7 mm SL, 2 c&s, 27.6–31.8 mm SL. *Hoplisoma armatum*: BMNH 1867.6.13.51, lectotype of *Callichthys armatus* Günther, 1868, 42.1 mm SL. *Hoplisoma atropersonatum*: USNM 204359, holotype of *Corydoras atropersonatus* Weitzman, Nijssen, 1970, 37.1 mm SL. *Hoplisoma benattii*: MZUSP 121671, holotype of *Corydoras benattii*, 25.4 mm SL. *Hoplisoma boehlkei*: ANSP 148097, holotype of *Corydoras boehlkei* Nijssen, Isbrücker, 1982, 23.6 mm SL. *Hoplisoma bondi*: ROM 66202, 134 7, 33.8–39.9 mm SL, 3 c&s, 36.7–38.6 mm SL. *Hoplisoma brevirostre*: LBP 3080, 10, 23.8–27.7 mm SL, 3 c&s, 25.8–27.9 mm SL. *Hoplisoma burgessi*: USNM 288461, 2, 43.7–44.8 mm SL, paratypes of *Corydoras burgessi*. *Hoplisoma carlae*: NUP 711, 1, 47.9 mm SL; NUP 4425, 1 c&s, 45.0 mm SL. *Hoplisoma colossus*: MNRJ 54421, holotype of *Corydoras colossus*, 44.5 mm SL; CITL 928, 1 of 3, 42.2 mm SL, 2 c&s of 3, 43.1–48.4 mm SL, paratypes of *Corydoras colossus*. *Hoplisoma coppenamense*: USNM 202129, 5, 33.0–35.8 mm SL, paratypes of *Corydoras coppenamensis* Nijssen, 1970. *Hoplisoma davidsandsi* Black, 1987: MZUSP 110066, 40 4, 36.0–41.9 mm SL, 2 c&s specimens, 40.9–42.1 mm SL. *Hoplisoma diphyes*: ANSP 169756, 2, 40.7–43.1 mm SL. *Hoplisoma ehrhardti*: NUP 11255, 15, 36.5–46.8 mm SL. *Hoplisoma eversi*: MNRJ 43195, holotype of *Corydoras eversi*, 44.5 mm SL. *Hoplisoma flaveolum*: MZUSP 424, holotype of *Corydoras flaveolus* Ihering, 1911, 33.4 mm SL. *Hoplisoma gossei*: MZUSP 38977, 6, 48.4–53.4 mm SL, paratypes of *Corydoras gossei* Nijssen, 1972. *Hoplisoma granti*: MNRJ 51193, holotype of *Corydoras granti*, 48.4 mm SL. *Hoplisoma griseum*: MZUSP 108896, 13, 4, 31.5–36.2 mm SL, 2 c&s, 30.6–34.5 mm SL. *Hoplisoma gryphus*: MNRJ 40770, holotype of *Corydoras gryphus* Tencatt, Britto & Pavanelli, 2014, 32.3 mm SL; NUP 14676, 3 c&s, 27.7–32.4 mm SL, paratypes. *Hoplisoma guianense*: USNM 204218, 2, 26.0–32.0 mm SL, paratypes of *Corydoras guianensis* Nijssen, 1970. *Hoplisoma hypnos*: MNRJ 53288, holotype of *Corydoras hypnos*, 31.7 mm SL. *Hoplisoma julii*: NUP 16225, 1, 46.8 mm SL. *Hoplisoma kanei*: MZUSP 52489, holotype of *Corydoras kanei*, 36.6 mm SL. *Hoplisoma knaacki*: MUSM 52730, holotype of *Corydoras knaacki* Tencatt & Evers, 2016, 35.6 mm SL. *Hoplisoma lacrimostigmata*: MNRJ 40725, holotype of *Corydoras lacrimostigmata* Tencatt, Britto & Pavanelli, 2014, 31.8 mm SL; NUP 14657, 3 c&s, 30.9–34.5 mm SL, paratypes. *Hoplisoma longipinne*: AI 221, holotype of *Corydoras longipinnis* Knaack, 2007,

59.5 mm SL; NUP 14440, 2 c&s, 29.9–33.4 mm SL. *Hoplisoma loretoense*: ANSP 121620, 32, 17.3–32.7 mm SL, paratypes of *Corydoras loretoensis* Nijssen, Isbrücker, 1986. *Hoplisoma loxozonum*: ANSP 150170, holotype of *Corydoras loxozonus* Nijssen, Isbrücker, 1983, 34.6 mm SL. *Hoplisoma lymnades*: MNRJ 15765, 6, 15.8–17.7 mm SL, 2 c&s, 18.1–18.4 mm SL; MNRJ 40186, holotype of *Corydoras lymnades* Tencatt, Vera-Alcaraz, Britto & Pavanelli, 2013, 29.7 mm SL. *Hoplisoma melanistium*: BMNH 1864.1.21.86, lectotype of *Corydoras melanistius*, 35.0 mm SL. *Hoplisoma micracanthus*: BMNH 1897.1.27.8, lectotype of *Corydoras micracanthus* Regan, 1912, 33.7 mm SL. *Hoplisoma multimaculatum*: MCP 29025, 2, 20.1–25.4 mm SL. *Hoplisoma nattereri*: MZUSP 110255, 31 4, 32.0–32.8 mm SL, 2 c&s, 32.3–34.4 mm SL. *Hoplisoma noxium*: MNRJ 55759, holotype of *Hoplisoma noxium*, 54.8 mm SL. *Hoplisoma oiapoquense*: USNM 205868, 2, 25.9–35.0 mm SL, paratypes of *Corydoras oiapoquensis*. *Hoplisoma osteocarus*: USNM 157367, 1, 25.1 mm SL, paratype of *Corydoras osteocarus* Böhlke, 1951. *Hoplisoma paleatum*: BMNH 1917.7.14.18, lectotype of *Callichthys paleatus* Jenyns, 1842, 30.0 mm SL; NRM 54230, 1, 53.5 mm SL. *Hoplisoma panda*: BMNH 1969.7.15.8, holotype of *Corydoras panda* Nijssen & Isbrücker, 1971, 38.9 mm SL; ROM 55815, 6, 26.5–39.7 mm SL. *Hoplisoma parallelum*: MZUSP 45716, holotype of *Corydoras parallelus*, 47.4 mm SL. *Hoplisoma pavanelliae*: MNRJ 43317, holotype of *Corydoras pavanelliae*, 45.1 mm SL. *Hoplisoma polystictum*: BMNH 1895.5.17.62, lectotype of *Corydoras polystictus*, 27.5 mm SL; CITL 1590, 3 c&s, 30.7–35.8 mm SL. *Hoplisoma psamathos*: MNRJ 53289, holotype of *Corydoras psamathos*, 29.4 mm SL. *Hoplisoma potaroense*: ROM 61526, 3 of 15, 35.0–44.8 mm SL, 2 c&s, 32.6–35.1 mm SL. *Hoplisoma punctatum*: ZMB 3149, lectotype of *Cataphractus punctatus* Bloch, 1794, 41.7 mm SL. *Hoplisoma simile*: LBP 10648, 7, 21.4–34.3 mm SL. *Hoplisoma surinamense*: USNM 204223, 2, 29.1–34.3 mm SL, paratypes of *Corydoras surinamensis*. *Hoplisoma tenebrosum*: MNRJ 55757, holotype of *Hoplisoma tenebrosum*, 52.5 mm SL. *Hoplisoma thanatos*: MNRJ 53287, holotype of *Corydoras thanatos*, 33.2 mm SL. *Hoplisoma trilineatum*: ANSP 8294, lectotype of *Corydoras trilineatus*, 31.8 mm SL; MZUSP 30857, 25, 3, 40.9–44.1 mm SL, 2 c&s, 44.2–43.8 mm SL. *Hoplisoma tukano*: MZUSP 82100, holotype of *Corydoras tukano* Britto & Lima, 2003, 40.9 mm SL. *Hoplisoma urucu*: MNRJ 32446, 4, 25.9–27.3 mm SL, paratypes of *Corydoras urucu* Britto, Wosiacki & Montag, 2009. *Hoplisoma weitzmani*: USNM 206018, 1, 38.5 mm SL, paratype of *Corydoras weitzmani* Nijssen, 1971. *Hoplisoma xinguense*: USNM 205870, 1, 27.9 mm SL, paratype of *Corydoras xinguensis*.

ACKNOWLEDGMENTS

This work is dedicated to the members of the Greater Pittsburgh Aquarium Society, Inc., for making the expedition to Jacareacanga, Pará, possible. The Universidade Federal de Mato Grosso (UFMT), and Universidade Federal de Mato Grosso do Sul (UFMS) provided logistical support. The authors are grateful to Carla Pavanelli (NUP), Carlos Lucena and Margarete Lucena (MCP), Cláudio Oliveira (LBP), Aléssio Datovo, Michel Gianeti, and Osvaldo Oyakawa (MZUSP), Kris Murphy, Sandra Raredon and Jeffrey Clayton (USNM), Mark Sabaj and Mariangeles Arce (ANSP), James Maclaine and Oliver Crimmen (BMNH), and Otávio Froehlich (*in memoriam*) (ZUFMS) for hosting museum visits and loaning of material. To Emanuel Neuhaus (MNRJ), Francisco Severo-Neto and Thomaz Sinani (ZUFMS-PIS), Carlos Lucena (MCP), Cláudio Oliveira, Ricardo Britzke, Fábio Roxo, Bruno Melo and Gabriel Silva (LBP), and Willian Ohara, Vinícius Espíndola and Túlio Teixeira (MZUSP) for generously welcoming LFCT during museum visits. To Fernando Vaz-de-Mello and Jorge Arias from the Laboratório de Scarabaeoidologia (UFMT) for allowing the use and general support of the photomontage equipment Leica M205C (subproject EECBio UFMT/

Finep #01.12.0359.00), respectively. To Wei-Chieh Tseng, Hans Evers, Ian Fuller and Haakon Haagensen for sending photographs in life of the new species. To the members of the fish keeping groups *Corydoras* World (United Kingdom), Catfish Study Group (United Kingdom), Internationale Gemeinschaft Barben Salmler Schmerlen Welse e.V. (Germany), Potomac Valley Aquarium Society (United States of America), Ohio Cichlid Association (USA), Greater Pittsburgh Aquarium Society, Inc. (USA), and All Oddball Aquatics (USA) for the invaluable support to LFCT.

REFERENCES

- **Alexandrou MA, Oliveira C, Maillard M, McGill RAR, Newton J, Creer S *et al*.** Competition and phylogeny determine community structure in Müllerian co-mimics. Nature. 2011; 469:84–89. https://doi.org/10.1038/nature09660
- **Amiri MH, Shaheen HM.** Chromatophores and color revelation in the blue variant of the Siamese fighting fish (*Betta splendens*). Micron. 2012; 43(2–3):159–69. https://doi.org/10.1016/j.micron.2011.07.002
- **Andrade P, Carneiro M.** Pterin-based pigmentation in animals. Biol Lett. 2021; 17(8):20210221. https://doi.org/10.1098/rsbl.2021.0221
- **Arratia G, Gayet M.** Sensory canals and related bones of Tertiary siluriform crania from Bolivia and North America and comparison with recent forms. J Vertebr Paleontol. 1995; 15:482–505.
- **Bagnara JT, Fernandez PJ, Fujii R.** On the blue coloration of vertebrates. Pigment Cell Res. 2007; 20(1):14–26. https://doi.org/10.1111/j.1600-0749.2006.00360.x
- **Ballen GA, de Pinna, MC.** A standardized terminology of spines in the order Siluriformes (Actinopterygii: Ostariophysi). Zool J Linn Soc. 2021; 194(2):601–25.
- **Bentley RF, Grant S, Tencatt LFC.** A new arc-striped species of *Corydoras* Lacépède, 1803 (Teleostei: Callichthyidae) from the Peruvian Amazon. Zootaxa. 2021; 4948(2):184–200.
- **Britto MR.** Phylogeny of the subfamily Corydoradinae Hoedeman, 1952 (Siluriformes: Callichthyidae), with a definition of its genera. PNAS. 2003; 153:119–54. https://doi.org/10.1635/0097-3157(2003)153[0119:POTSCH]2.0.CO;2
- **Britto MR, Lima FCT.** *Corydoras tukano*, a new species of Corydoradine catfish from the rio Tiquié, upper rio Negro basin, Brazil (Ostariophysi: Siluriformes: Callichthyidae). Neotrop Ichthyol. 2003; 1(2):83–91. https://doi.org/10.1590/S1679-62252003000200002
- **Britto MR, Tencatt LFC, Dopazo M, Santos SA, Ferreira KCF, Reis RE.** Phylogeny and classification of the family Callichthyidae (Armored catfishes). In: Arratia G, Reis RE, editors. Catfishes, a highly diversified group, volume 2, evolution and phylogeny. Boca Raton: CRC Press, Taylor & Francis Group, Science Publishers; 2025. p.155–72.
- **Castilhos ZC, Bidone ED, Lacerda LD.** Increase of the background human exposure to mercury through fish consumption due to gold mining at the Tapajós River region, Pará State, Amazon. Bull Environ Contam Toxicol. 1998; 61(2):202–09.
- **Chatelain P, Elias M, Fontaine C, Villemant C, Dajoz I, Perrard A.** Müllerian mimicry among bees and wasps: a review of current knowledge and future avenues of research. Biol Rev. 2023; 98(4):1310–28. https://doi.org/10.1111/brv.12955
- **Clothier J, Lythgoe JN.** Light-induced colour changes by the iridophores of the Neon tetra, *Paracheirodon innesi*. J Cell Sci. 1987; 88(5):663–68.
- **Cott HB.** Adaptive Coloration in Animals. Methuen: Oxford University Press; 1940.
- **Crompton P, Ventura AM, Souza JM, Santos E, Strickland GT, Silbergeld E.** Assessment of mercury exposure and malaria in a Brazilian Amazon riverine community. Environ Res. 2002; 90(2):69–75. https://doi.org/10.1006/enrs.2002.4358

- **Dias AC, Tencatt LFC, Roxo FF, Silva GC, Santos SA, Britto MR *et al*.** Phylogenomic analyses in the complex Neotropical subfamily Corydoradinae (Siluriformes: Callichthyidae) with a new classification based on morphological and molecular data. Zool J Linn Soc. 2025; 203(3):zlae053. https://doi.org/10.1093/zoolinnean/zlae053
- **Doucet SM, Meadows MG.** Iridescence: a functional perspective. J R Soc Interface. 2009; 6(suppl. 2):S115–32.
- **Fricke R, Eschmeyer WN, Fong JD.** Eschmeyer's catalog of fishes: species by family/subfamily [Internet]. San Francisco: California; 2026. Available from: https://researcharchive.calacademy.org/research/ichthyology/catalog/SpeciesByFamily.asp
- **Fujii R.** 6 Chromatophores and pigments. Fish Physiol. 1969; 3:307–53.
- **Fuller IAM, Evers HG.** Identifying Corydoradine Catfish, second edition. Kidderminster: Ian Fuller Enterprises; 2024.
- **Ghosh S, Yu CL, Ferraro DJ, Sudha S, Pal SK, Schaefer WF *et al*.** Blue protein with red fluorescence. PNAS. 2016; 113(41):11513–18. https://doi.org/10.1073/pnas.1525622113
- **Grant S.** Chronic recurrent colour change in Hypostominae (Loricariidae). JCSG. 2019; 20(2):11–20.
- **Gray SM, Dill LM, Tantu FY, Loew ER, Herder F, McKinnon JS.** Environment-contingent sexual selection in a colour polymorphic fish. Proc Biol Sci. 2008; 275(1644):1785–91. https://doi.org/10.1098/rspb.2008.0283
- **Hamied A, Alnedawy Q, Correia A, Hacker C, Ramsdale M, Hashimoto H *et al*.** Identification and characterization of highly fluorescent pigment cells in embryos of the Arabian killifish (*Aphanius dispar*). iScience. 2020; 23(11):101674.
- **Huysentruyt F, Adriaens D.** Descriptive osteology of *Corydoras aeneus* (Siluriformes: Callichthyidae). Cybium. 2005; 29:261–73.
- **International Union for Conservation of Nature (IUCN). Standards and Petitions Committee.** Guidelines for using the IUCN Red List Categories and Criteria. Version 16. 2024. Available from: https://www.iucnredlist.org/documents/RedListGuidelines.pdf
- **Jacobs GH.** Ultraviolet vision in vertebrates. Am Zool. 1992; 32(4):544–54.
- **Junior CDMB, Carvalho LG.** Transformations in artisanal and small-scale gold mining work and production structures in the Tapajós region of Brazil's amazon. Resour Policy. 2023; 83:103597. https://doi.org/10.1016/j.resourpol.2023.103597
- **Kiehl E, Rieger C, Greven H.** Axillary gland secretions contribute to the stress-induced discharge of a bactericidal substance in *Corydoras sterbai* (Callichthyidae, Siluriformes). Verh Ges Ichthyol. 2006; 5:111–15.
- **Kimura T, Nagao Y, Hashimoto H, Yamamoto-Shiraishi Y, Yamamoto S, Yabe T *et al*.** Leucophores are similar to xanthophores in their specification and differentiation processes in medaka. PNAS. 2014; 111(20):7343–48. https://doi.org/10.1073/pnas.1311254111
- **Leclercq E, Taylor JF, Migaud H.** Morphological skin colour changes in teleosts. Fish Fish. 2010; 11:159–93.
- **Ligon RA, McCartney KL.** Biochemical regulation of pigment motility in vertebrate chromatophores: a review of physiological color change mechanisms. Curr Zool. 2016; 62(3):237–52. https://doi.org/10.1093/cz/zow051
- **Lobo FL, Costa MPF, Novo EMLM.** Time-series analysis of Landsat-MSS/TM/OLI images over Amazonian waters impacted by gold mining activities. Remote Sens Environ. 2015; 157:170–84. https://doi.org/10.1016/j.rse.2014.04.030
- **Lundberg JG.** The evolutionary history of North American catfishes, family Ictaluridae. [PhD Thesis]. Michigan: The University of Michigan; 1970.

- **Marinho MMF, Dagosta FCP, Camelier P, Oyakawa OT.** A name for the 'blueberry tetra', an aquarium trade popular species of *Hyphessobrycon* Durbin (Characiformes, Characidae), with comments on fish species descriptions lacking accurate type locality. J Fish Biol. 2016; 89(1):510–21. https://doi.org/10.1111/jfb.12991
- **Marshall JN.** Communication and camouflage with the same 'bright' colours in reef fishes. Phil Trans R Soc Lond. 2000; 355(1401):1243–48. https://doi.org/10.1098/rstb.2000.0676
- **McDowall RM.** Caudal skeleton in *Galaxias* and allied genera (Teleostei: Galaxiidae). Copeia. 1999; 1999(4):932–39. https://doi.org/10.2307/1447968
- **Monod T.** Le complèxe urophore des poissons téléostéens. Mem Inst Franç Afrique Noire. 1968; 81:1–705.
- **Nijssen H, Isbrücker IJH.** *Aspidoras virgulatus* n. sp., a plated catfish from Espírito Santo, Brazil (Pisces, Siluriformes, Callichthyidae). Bull Zool Mus Univ Amsterdam. 1980; 7:133-39.
- **Parker GH.** Animal color changes and their neurohumours, first edition. Cambridge: Cambridge University Press; 1948.
- **Reis RE.** Revision of the Neotropical catfish genus *Hoplosternum* (Ostariophysi: Siluriformes: Callichthyidae), with the description of two new genera and three new species. Ichthyol Explor Freshw. 1997; 7(4):299–326.
- **Reis RE.** Anatomy and phylogenetic analysis of the Neotropical callichthyid catfishes (Ostariophysi, Siluriformes). Zool J Linn Soc. 1998; 124(2):105–68. https://doi.org/10.1111/j.1096-3642.1998.tb00571.x
- **Reis RE.** Family Callichthyidae (Armored catfishes). In: Reis RE, Kullander SO, Ferraris Jr. CJ, editors. Check list of the freshwater fishes of South and Central America. Porto Alegre: Edipucrs; 2003. p.291–309.
- **Sabaj MH.** Codes for Natural History Collections in Ichthyology and Herpetology. (online supplement). Version 10. 2026. Available from: https://www.asih.org/resources/standard-symbolic-codes
- **Sadovy Y, Randall JE, Rasotto MB.** Skin structure in six dragonet species (Gobiesociformes; Callionymidae): interspecific differences in glandular cell types and mucus secretion. J Fish Biol. 2005; 66(5):1411–18. https://doi.org/10.1111/j.0022-1112.2005.00692.x
- **Schaefer SA.** Homology and evolution of the opercular series in the loricarioid catfishes (Pisces: Siluroidei). J Zool. 1988; 214(1):81–93. https://doi.org/10.1111/j.1469-7998.1988.tb04988.x
- **Schaefer SA, Aquino AE.** Postotic laterosensory canal and pterotic branch homology in catfishes. J Morphol. 2000; 246(3):212–27. https://doi.org/10.1002/1097-4687(200012)246:3%3C212::AID-JMOR5%3E3.0.CO;2-S
- **Schaefer WF, Schmitz MH, Blazer VS, Ehlinger TJ, Berges JA.** Localization and seasonal variation of blue pigment (sandercyanin) in walleye (*Sander vitreus*). Can J Fish Aquat Sci. 2015; 72(2):281–89. https://doi.org/10.1139/cjfas-2014-0139
- **Sköld HN, Aspengren S, Wallin M.** Rapid color change in fish and amphibians – function, regulation, and emerging applications. Pigment Cell Melanoma Res. 2013; 26(1):29–38. https://doi.org/10.1111/pcmr.12040
- **Slobodian V, Pastana MNL.** Description of a new *Pimelodella* (Siluriformes: Heptapteridae) species with a discussion on the upper pectoral girdle homology of Siluriformes. J Fish Biol. 2018; 93(5):901–16. https://doi.org/10.1111/jfb.13795
- **Spadella MA, Desan SP, Henriques TCBPO, Oliveira C.** Variation in male reproductive system characters in Corydoradinae (Loricarioidei: Callichthyidae) reflects the occurrence of different lineages in this subfamily. Neotrop Ichthyol. 2017; 15(1):e160039. https://doi.org/10.1590/1982-0224-20160039
- **Springer VG, Johnson GD.** Use and advantages of ethanol solution of alizarin red S dye for staining bone in fishes. Copeia. 2000; 2000(1):300–01. https://doi.org/10.1643/0045-8511(2000)2000[0300:UAAOES]2.0.CO;2
- **Taylor WR, Van Dyke GC.** Revised procedures for staining and clearing small fishes and other vertebrates for bone and cartilage study. Cybium. 1985; 9(2):107–19.

- **Tencatt LFC, Britto MR, Isbrücker IJH, Pavanelli CS.** Taxonomy of the armored catfish genus *Aspidoras* (Siluriformes: Callichthyidae) revisited, with the description of a new species. Neotrop Ichthyol. 2022b; 20(3):e220040. https://doi.org/10.1590/1982-0224-2022-0040
- **Tencatt LFC, Carvalho V, Silva HP, Britto MR.** A new striped *Osteogaster* (Siluriformes: Callichthyidae) from the Madeira and Tapajós river basins, Brazil, with a new generic diagnosis and an identification key to the species of *Osteogaster*. Neotrop Ichthyol. 2025b; 23(2):e240134. https://doi.org/10.1590/1982-0224-2024-0134
- **Tencatt LFC, Couto OLP, Santos SA, Sousa LM.** A new long-snouted *Corydoras* (Siluriformes: Callichthyidae) from the rio Xingu and rio Tapajós basins, Brazilian Amazon. Neotrop Ichthyol. 2024a; 22(1):e230112. https://doi.org/10.1590/1982-0224-2023-0112
- **Tencatt LFC, Gomes VDC, Evers HG.** A new species of *Corydoras* (Siluriformes: Callichthyidae) from the rio Madre de Dios basin, Peruvian Amazon, with comments on *Corydoras aeneus* identity. Neotrop Ichthyol. 2023a; 21(2):e230023. https://doi.org/10.1590/1982-0224-2023-0023
- **Tencatt LFC, Grant S, Bentley RF.** A new color-changing species of *Corydoras* (Siluriformes: Callichthyidae) from the rio Jutaí, Brazilian Amazon. Neotrop Ichthyol. 2023b; 21(4):e230105. https://doi.org/10.1590/1982-0224-2023-0105
- **Tencatt LFC, Hercos AP, Carvalho V, Santos SA, Britto MR.** A new *Corydoras* (Siluriformes: Callichthyidae) from the rio Tefé basin, Brazilian Amazon, with comments on the taxonomic status of *Corydoras orcesi* and a discussion on the mouth morphology in Corydoradinae. Neotrop Ichthyol. 2026; 24(2):e250146. https://doi.org/10.1590/1982-0224-2025-0146
- **Tencatt LFC, Ohara WM, Carvalho V, Grant S, Britto M.** Two exquisite new species of *Hoplisoma* (Siluriformes: Callichthyidae) from the rio Tapajós basin, Brazil, with a discussion on the morphology of the mesethmoid within Corydoradinae. Neotrop Ichthyol. 2025a; 23(1):e240100. https://doi.org/10.1590/1982-0224-2024-0100
- **Tencatt LFC, Ohara WM, Sousa LM, Britto MRD.** Science and hobby joining forces for the discovery of three new *Corydoras* (Siluriformes: Callichthyidae) from the rio Tapajós basin, Brazil, with comments on *Corydoras* sp. CW111. Neotrop Ichthyol. 2022a; 20(3):e220070. https://doi.org/10.1590/1982-0224-2022-0070
- **Tencatt LFC, Ruiz-Tafur M, Chuctaya J.** A new masked *Corydoras* (Siluriformes: Callichthyidae) from the Itaya and Nanay river basins, Peruvian Amazon. Neotrop Ichthyol. 2024b; 22(2):e240016. https://doi.org/10.1590/1982-0224-2024-0016
- **Tencatt LFC, Santos SA, Evers HG, Britto MR.** *Corydoras fulleri* (Siluriformes: Callichthyidae), a new catfish species from the rio Madeira basin, Peru. J Fish Biol. 2021; 99(2):614–28. https://doi.org/10.1111/jfb.14750
- **Umbers KDL.** On the perception, production and function of blue colouration in animals. J Zool. 2013; 289(4):229–42. https://doi.org/10.1111/jzo.12001
- **Vera-Alcaraz HS.** Relações filogenéticas das espécies da família Callichthyidae (Ostariophysi, Siluriformes). [PhD Thesis]. Porto Alegre: Pontifícia Universidade Católica do Rio Grande do Sul; 2013. Available from: https://tede2.pucrs.br/tede2/handle/tede/263
- **Zarske A.** *Knodus borki* sp. n. – ein neuer Salmler aus Peru mit einer ergänzenden Beschreibung von *Boehlkea fredcochui* Géry, 1966 (Teleostei: Characiformes: Characidae). Vertebr Zool. 2008; 58(2):159–71. https://doi.org/10.3897/vz.58.e30929
- **Zhao N, Ge X, Jiang K, Huang J, Wei K, Sun C *et al*.** Ultrastructure and regulation of color change in blue spots of leopard coral trout *Plectropomus leopardus*. Front Endocrinol. 2022; 13:984081. https://doi.org/10.3389/fendo.2022.984081

AUTHORS' CONTRIBUTION

Luiz Fernando Caserta Tencatt: Conceptualization, Data curation, Formal analysis, Funding acquisition, Investigation, Methodology, Project administration, Resources, Supervision, Validation, Visualization, Writing original draft, Writing-review and editing.

Willian Massaharu Ohara: Data curation, Funding acquisition, Investigation, Methodology, Project administration, Resources, Visualization, Writing-review and editing.

Vandergleison de Carvalho: Data curation, Formal analysis, Investigation, Methodology, Writing-review and editing.

Steven Grant: Data curation, Investigation, Visualization, Writing original draft, Writing-review and editing.

Marcelo R. Britto: Data curation, Investigation, Methodology, Supervision, Validation, Visualization, Writing-review and editing.

FUNDING INFORMATION

The Coordenação de Aperfeiçoamento de Pessoal de Nível Superior (CAPES) provided financial support to VCG (proc. #88887.902472/2023–00). The Conselho Nacional de Desenvolvimento Científico e Tecnológico (CNPq) provided financial support to MRB (proc. #306059/2024-0).

ETHICAL STATEMENT

Specimens were collected and/or transported under the permanent licenses for the collection of zoological material #65628–5 to WMO and #85671–1 to LFCT, from the Instituto Chico Mendes de Conservação da Biodiversidade, Sistema de Autorização e Informação em Biodiversidade (ICMBio/SISBIO).

DATA AVAILABILITY STATEMENT

The authors confirm that the data supporting the findings of this study are available within the article.

AI STATEMENT

The authors did not use any AI-assisted technologies in the creation of this manuscript or its figures.

COMPETING INTERESTS

The author declares no competing interests.

PEER REVIEW REPORT

Reviewers:

Anonymous reviewer #1

Anonymous reviewer #2

The peer review report is available at: Neotropical Ichthyology

HOW TO CITE THIS ARTICLE

- **Tencatt LFC, Ohara WM, Carvalho V, Grant S, Britto MR.** Two co-mimic new species of Corydoradinae catfishes (Siluriformes: Callichthyidae) from the rio Tapajós basin, Brazil, with a discussion on their color pattern. Neotrop Ichthyol. 2026; 24(4):e260077. https://doi.org/10.1590/1982-0224-2026-0077

Neotropical Ichthyology

OPEN ACCESS

This is an open access article under the terms of the Creative Commons Attribution License, which permits use, distribution and reproduction in any medium, provided the original work is properly cited.

Distributed under
Creative Commons CC-BY 4.0

© 2026 The Authors.
Published by SBI

Official Journal of the
Sociedade Brasileira de Ictiologia

SBI